IOPscience iopscience.iop.org

Home Search Collections Journals About Contact us My IOPscience

Magnetism in nanoparticles: tuning properties with coatings

This content has been downloaded from IOPscience. Please scroll down to see the full text.

2013 J. Phys.: Condens. Matter 25 484006

(http://iopscience.iop.org/0953-8984/25/48/484006)

View the table of contents for this issue, or go to the journal homepage for more

Download details:

IP Address: 147.96.1.236
This content was downloaded on 08/11/2013 at 12:31

Please note that terms and conditions apply.

J. Phys.: Condens. Matter **25** (2013) 484006 (21pp) doi:10.1088/0953-8984/25/48/484006

TOPICAL REVIEW

Magnetism in nanoparticles: tuning properties with coatings

Patricia Crespo[1,2], Patricia de la Presa[1,2], Pilar Marín[1,2], Marta Multigner[1], José María Alonso[1], Guillermo Rivero[1,2], Félix Yndurain[3], José María González-Calbet[1,4] and Antonio Hernando[1,2]

[1] Instituto de Magnetismo Aplicado, PO Box 155, E-28230 Las Rozas, Spain
[2] Facultad Ciencias Físicas, Departamento Física de Materiales, Universidad Complutense de Madrid, Spain
[3] Departamento Fis Mat Condensada, Universidad Autonoma Madrid, E-28049 Madrid, Spain
[4] Facultad de Químicas, Departamento Química Inorgánica, Universidad Complutense de Madrid, E-28040 Madrid, Spain

E-mail: antonio.hernando@externos.adif.es

Received 31 January 2013, in final form 15 May 2013
Published 7 November 2013
Online at stacks.iop.org/JPhysCM/25/484006

Abstract
This paper reviews the effect of organic and inorganic coatings on magnetic nanoparticles. The ferromagnetic-like behaviour observed in nanoparticles constituted by materials which are non-magnetic in bulk is analysed for two cases: (a) Pd and Pt nanoparticles, formed by substances close to the onset of ferromagnetism, and (b) Au and ZnO nanoparticles, which were found to be surprisingly magnetic at the nanoscale when coated by organic surfactants. An overview of theories accounting for this unexpected magnetism, induced by the nanosize influence, is presented. In addition, the effect of coating magnetic nanoparticles with biocompatible metals, oxides or organic molecules is also reviewed, focusing on their applications.

(Some figures may appear in colour only in the online journal)

Contents

1. Introduction

When the particle sizes of materials are reduced to the nanoscale level, their physical properties change as particle dimensions (at least one dimension, as in the case of thin films) become comparable to the characteristic lengths of certain physical phenomena. Consequently, nanostructures exhibit properties that are different from their bulk counterparts, thus nanomaterials are attracting a great deal of interest due to their potential uses in different disciplines such magnetic recording [1–3], magnetic resonance imaging

 © 2013 IOP Publishing Ltd Printed in the UK & the USA

and related technologies [4–6], catalysis [7, 8], analytical chemistry [9, 10], and biomedical applications [11–13].

By decreasing particle size to the nanoscale, new magnetic phenomena appear [14, 15]. As is known, the spacing between adjacent conduction energy states increases with a decrease in the volume of the particle; therefore, changes in the electronic energy spectrum take place as the particle size decreases and the continuum that describes the band of allowed energy states of the bulk material becomes a discrete set of states for nanoparticles (NPs). In particular, the density of states $N(\varepsilon_F)$ at the Fermi level, the parameter that governs electronic properties, is strongly affected by the nanoscale and, therefore, the properties of NPs differ significantly from bulk-like systems of the same material [16, 17]. A nice example of this size effect can be found in the work of Billas *et al* [18], which reports an increase in magnetization as the number of atoms in clusters of Fe, Ni and Co atoms is reduced.

Local enhancement of $N(\varepsilon_F)$ could promote ferromagnetism in nanoscale clusters of systems that do not exhibit ferromagnetic ordering in the bulk. The factors that increase $N(\varepsilon_F)$ are (i) the confinement effects associated with a reduced coordination number [19, 20]; (ii) local symmetry changes due to the effect of vacancies [21] or by increasing the percentage of atoms at the grain boundaries or interfaces; and (iii) changes of the lattice constant at the surface that induce a narrowing of the d band. For instance, in the case of Pd, the onset of ferromagnetic behaviour should take place at a lattice expansion of about 5%, according to theoretical calculations [22–24]. Other examples are the shift of the Curie temperature due to changes in the lattice parameter [25]. Mössbauer spectroscopy studies on nanophase Fe have shown two sextets, bulk and surface, also due to lattice constant changes [26, 27]. The local enhancement of $N(\varepsilon_F)$ is responsible, for instance, for the occurrence of ferromagnetism in Rh clusters with 9–31 atoms [28]. Also, clusters of Pd and Pt with particle sizes below 2 nm have been reported to exhibit ferromagnetism [29, 30].

Another aspect that should be considered, when dealing with NPs, is the enormous ratio of surface-to-volume numbers of atoms, which has important consequences. Whereas for an ideal solid the surface can be thought of as a defect, for NPs the surface atoms have a larger contribution as the particle size decreases. At the nanoscale, translational symmetry is broken, giving rise to different local physical properties. Electronic states change to surface states, magnetic anisotropy is modified to surface anisotropy and crystalline short-range order undergoes a sharp discontinuity as the surface is approached from the internal volume. Therefore, all the physical properties sensitive to short-range order exhibit surface behaviour that is different from that observed in the volume.

The high surface-to-volume ratio makes NPs highly sensitive to the environment. In general, metallic NPs are chemically very active and, in most cases, become surface oxidized when exposed to air. Thus, it is necessary to create a coating for stabilizing the particles, which can be made of organic or inorganic compounds. In some cases, the coating merely acts as a barrier protecting the NP against external agents, but in other cases it can drastically affect the electronic properties of the NP.

The modification of the NP surface by means of bonding specific molecules to the surface atoms plays a crucial role in the minimization of the energy and, consequently, in the stabilization of the system. Capping has been demonstrated as a valid method for tuning physical properties at the nanoscale.

Due to the large number of atoms at the NP surface, the sample as a whole is dramatically sensitive to the atoms coating the particle. This influence has been experimentally found to be as important as that previously discussed above, as for instance through the effect of the coating on the magnetic properties. It seems to be obvious that covalent bonds of surface atoms are going to dramatically affect their electronic and, consequently, their optical and magnetic properties. In other words, the extremely sensitive electronic structure at the nanoscale will also be deeply modified by chemical bonding of the atoms. Note that the covalent bond of the surface atoms to the coating atoms gives rise to unusual types of chemical compounds that are very different to those in the bulk scale. For instance, Au NPs coated with thiol bonding are not expected to behave as gold sulfide, even though a large number of covalent Au–S bonds would be identical for both types of materials [31].

The experimental observation of a ferromagnetic-like behaviour in NPs of non-magnetic materials when they are coated by organic molecules has generated widespread interest. For instance, ferromagnetic behaviour up to room temperature (RT) in ZnO NPs has recently been reported, induced by capping with dodecylamine and dodecanethiol, whereas bulk ZnO is a semiconductor [32]. Ferromagnetism has also been reported in functionalized Pd NPs [33]. More surprising is the observation of ferromagnetic-like behaviour in Au NPs capped with thiol-derivatized molecules, because bulk gold is a diamagnetic material with a large diamagnetic susceptibility. Magnetic hysteresis up to RT was observed for the first time in alkanethiol-capped gold NPs using a superconducting quantum interference device (SQUID) magnetometer [34]. Several papers have since reported ferromagnetic behaviour in Au NPs capped with different thiol-derivatized molecules [35, 36]. The intrinsic magnetism has been corroborated by means of x-ray magnetic circular dichroism (XMCD) [37–40]. In addition to thiol-capped Au NPs, ferromagnetic-like behaviour has also been observed in capped Au NPs with other protective molecules [41–44] that do not bind to the Au surface by means of a thiol group.

Unfortunately, despite all the experimental work, the magnetic properties of these nanoscale clusters are currently not well understood. In order to account for the fact that magnetic hysteresis is observed at RT, it has been suggested that induced orbital magnetism in conduction electrons may come into play [45, 46]. The confinement of electrons in a 2D gas around the particle surface and the associated orbital magnetic moment is proposed to be the origin of the observed magnetic behaviour [47–49]. The main experimental results concerning induced ferromagnetic behaviour in NPs of Pd,

Pt and Au, as well as ZnO (semiconductor in bulk) will be reviewed in some detail.

On the other hand, coating of NPs with inorganic material enables the combination of two materials with different electronic properties, which can give rise to the enhancement of the chemical and physical properties of each, making these nanostructures useful in applications that would otherwise be inaccessible to their single component counterparts. These core–shell nanostructures offer a series of functionalities depending on the nature of the core and shell. For instance, metallic iron, which has large magnetic moment but oxidizes easily at the nanoscale, can be stabilized by passivation of the surface (an iron oxide shell) or by coating with gold or silica, making these NPs water stable and useful for biomedical applications. Thus, core/shell structures are multifunctional nanomaterials that can show enhanced optical, catalytic and magnetic properties compared to their individual single-component counterpart [50–56].

Besides, biological applications of magnetic NPs as new contrast agents for magnetic resonance (MR), diagnostic imaging and hyperthermia treatments of tumours requires a high degree of biocompatibility and colloidal stability. Organic coatings which improve the colloidal properties and samples biocompatibility could have a bearing on magnetic properties due to the formation of chemical bonds at the magnetic NP surface or the formation of different aggregates. Aggregation affects the spatially inhomogeneous particle distribution, leading to collective magnetization in order to decrease the magnetostatic energy. The effective field acting on a particle is the sum of the applied field and the field produced by the surrounding particles in the cluster. The organic coating can also affect the Brownian relaxation time due to its dependence on the hydrodynamic size, thus modifying the heating efficiency of magnetic NPs [57–61].

These nanostructures, exhibiting novel physical and chemical properties, are essential for future technological applications, but the material structure and interface coupling interactions must be finally well understood and adequately controlled [54]. In this paper, the coupling interactions between domains of coexisting materials, which are of relevance in defining multicomponent features, will be reviewed.

In summary, in this paper we describe the main experimental results obtained and reported over recent years in the field of surface-modified non-magnetic and magnetic NPs, emphasizing new experimental findings as well as the promising application of such nanostructured systems.

2. The onset of ferromagnetism at the nanoscale: the case of Pd and Pt NPs

From the point of view of nanoscale magnetism, one of the most attractive topics is the possibility of inducing a drastic modification of magnetic behaviour by reducing the particle size to nanoscale dimensions. In particular, the possibility of inducing ferromagnetic behaviour in normally non-magnetic systems is a hot topic in nanoscale magnetism.

Among those systems that have been reported to exhibit ferromagnetism at the nanoscale, 4d Pd and 5d Pt transition metals have attracted special attention since some theoretical calculations predicted ferromagnetic behaviour in low-dimensional systems, such as clusters or ultrathin films.

Bulk samples of Pd and Pt are paramagnetic; however, they exhibit enhanced Pauli paramagnetism. These two transition metals are close to ferromagnetic instability and consequently the appearance of traces of ferromagnetism at the NP scale does not seem extremely surprising. The experimentally detected magnetism in Pd [19, 20, 22, 30, 62–66] and Pt [29, 67–71] NPs has been interpreted in the framework of the overwhelming influence of the surface in nanosized particles.

The magnetic moment of a single NP is that obtained by adding the individual magnetic moments of the total number of electrons in the sample. If, in the absence of any applied magnetic field, this resultant moment is different from zero it is known as permanent magnetic moment. Ferromagnetic exchange interactions can promote the appearance of a spontaneous magnetic moment when the density of states at the Fermi level is sufficiently high. As the electronic energy structure is dramatically affected at nanometre sizes it is possible to observe permanent magnetism in NPs with compositions that are not magnetic in the bulk configuration. This is the case for the Pd NPs, as described below.

In particular, it has been demonstrated that small Pd NPs show ferromagnetic behaviour. Bulk Pd (fcc structure) presents a high paramagnetic susceptibility value and a high density of states at the Fermi level $N(\varepsilon_F) = 1.23\ \mathrm{eV}^{-1}/\mathrm{spin/atom}$, although not high enough to satisfy the Stoner criterion for ferromagnetism (for Pd the Stoner parameter is $J = 0.71$ eV, and therefore $N(\varepsilon_F)J = 0.87 < 1$). Surprisingly, in these NPs the magnetic behaviour is almost independent of T in the range 5–300 K, without superparamagnetic effects, as usually observed in NPs of bulk ferromagnetic materials. Giant orbital moments generated at the Fermi level that carry an associated giant orbital magnetic moment, up to that temperature for which k_BT becomes of the order of the distance in energy between the Fermi level and the first level above, could be the origin of this behaviour [47].

Experiments carried out by Taniyama *et al* [72] in 1997 demonstrated the appearance of a magnetic moment in Pd clusters with an average radius below 7 nm. Furthermore, these authors found ferromagnetic behaviour of Pd particles of 5.9 nm average radius with an atomic moment of 0.23 μ_B per surface atom. Later, Hori and collaborators reported unexpectedly large magnetic moments in Au and Pd NPs [73], with diameters ranging between 2.5 and 4 nm and protected with poly-*N*-vinyl-2-pyrrolidone (PVP) that works as a kind of matrix for the metal particles. In the latter, the magnetism of the Pd NPs was described by the size-dependent Stoner's enhancement model in combination with the surface effects.

Ferromagnetism up to RT of Pd NPs of 2.4 nm size was reported by Sampedro *et al* [30]. Pd NPs were obtained by a redox-controlled size-selective method, using $R_4N^+X^-$ as the surfactant in tetrahydrofuran [74]. Figure 1 shows the magnetization curves at low and high temperature. The thermal dependence of the magnetization is also shown. It is evident that the NPs exhibit a ferromagnetic-like behaviour at temperatures close to RT.

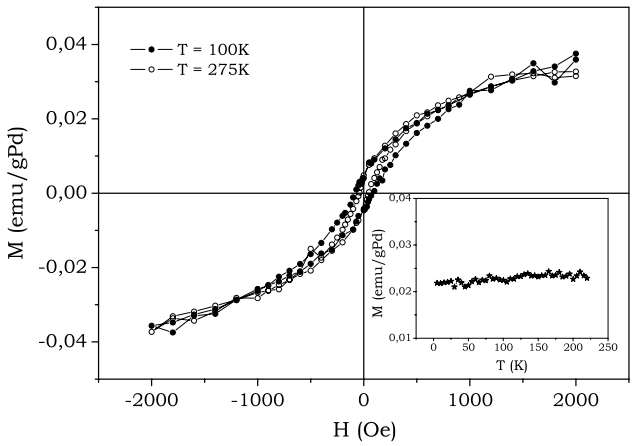

Figure 1. Magnetization curves of 2.4 nm Pd NPs measured at two different temperatures, 100 and 275 K. The inset shows the thermal dependence of the magnetization measured under an applied field of 1000 Oe. Notice that the magnetization exhibits almost no temperature dependence. (Reproduced with permission from [30]. Copyright 2003 American Physical Society.)

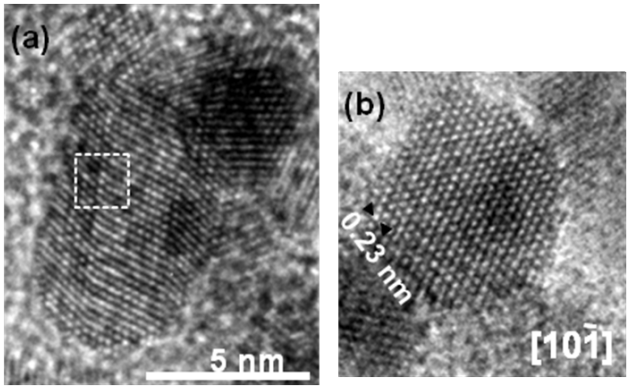

Figure 2. (a) HR-TEM image of a twinned Pt nanocrystal along the [10$\bar{1}$] zone; (b) HR-TEM image of a Pt NP with the fcc structure clearly visible.

Besides the careful magnetic characterization performed, high-resolution transmission electron microscopy (HR-TEM) studies showed the presence of twin boundaries in the NPs. The detailed analysis performed by HR-TEM on these NPs showed that most of these NPs exhibited twin boundaries in order to reduce their energy: fcc metals present a highly anisotropic surface energy. In a spherical NP, all the possible surface orientations are present. However, the presence of twin boundaries allows the most energetic orientations to be avoided, therefore reducing the surface energy. The twin boundary formation energy for fcc metals is quite low, and thus, in the energy balance, its formation reduces the total (surface plus volume) energy. In this situation, NPs exhibit a large fraction of atoms without cubic symmetry: those at the surface (representing a significant percentage of the total) and those close to the twin boundaries. The lack of cubic symmetry prevents the splitting of the d band into the t_{2g} and e_g sublevels and, therefore, it results in an overall narrowing of the band. Hence, in the vicinity of such atoms there is a higher density of states, which could be enough to satisfy the Stoner criterion. The strong surface energy anisotropy acts as the driving force for twinning in small Pd clusters.

Shinohara *et al* [62] also observed ferromagnetism in Pd NPs obtained by gas-evaporation. The Pd particles are found to have a magnetic heterostructure: the surface of the particle is ferromagnetic and the remainder is paramagnetic. The size dependence of the magnetic saturation component reveals that the ferromagnetic ordering occurs only on (100) facets of the particle. The onset of ferromagnetism is associated in this case with local enhancement of $N(\varepsilon_F)$ at the NP surface.

Later, Litran *et al* [33] conducted a study that demonstrated not only the influence of size effects on the magnetism of NPs but also the possibility of tuning the magnetic behaviour of Pd NPs with appropriate capping in a similar way to that reported by Crespo *et al* for Au NPs [34], as will be outlined below. Magnetization curves for all the samples showed hysteresis loops, demonstrating ferromagnetic or permanent magnetism in the NPs.

Among the late 4d transition metals, nanoscale Pd is not the only one that exhibits ferromagnetic behaviour. Ferromagnetism has also been reported in small carbon-coated platinum NPs (2–5 nm in size) [29]. In a similar way to that reported in the case of Pd NPs, electron microscopy studies confirmed that the NPs exhibit a large concentration of twin boundaries reducing the surface energy. Figure 2 shows representative HR-TEM images of Pt NPs.

The lack of cubic symmetry at the twin boundaries in combination with the large spin–orbit coupling of platinum could account for the huge magnetic anisotropy and, therefore, for the surprisingly high blocking temperature, above 300 K. More recently [67] it has been reported that thiol-coated Pt NPs showed ferromagnetism above RT. By means of XMCD measurements it was demonstrated that the ferromagnetism is inherent in the Pt. The appearance of ferromagnetism is mainly interpreted as being based on two mechanisms. One mechanism is the electronic band mechanism, i.e., the increase in the number of holes in the 5d band through charge transfer from the coating thiol and the change in electronic structure peculiar to the NP, with which the Stoner criterion for ferromagnetism is satisfied. The other one is orbital ferromagnetism due to electrons captured in the atomic-like orbital at the boundary of the surface region, which is coated with thiol molecules.

It can be concluded that the onset of ferromagnetism in systems that are close to ferromagnetic instability may be associated with a local increase of $N(\varepsilon_F)$ due to the overwhelming influence of the surface.

3. The onset of ferromagnetic-like behaviour in NPs: the effect of the organic coatings

3.1. Magnetic properties of Au NPs

Among those systems that exhibit a peculiar magnetic behaviour when they are reduced to the nanoscale, NPs of noble metals occupy an outstanding position. The observation of ferromagnetic-like behaviour in surface modified Au

[34, 39, 75], Ag [39, 76] and Cu [39] NPs have attracted much attention, not only for their potential in nanotechnology applications but also from the point of view of fundamental physics. It should be mentioned that the observation of ferromagnetism in Au NPs adds an important new functionality to this nanoscale system that, whether magnetic or not, exhibits broad potential in biology, catalysis and nanotechnology [10].

In this section we summarize the main results obtained from the experimental magnetic characterization of Au NPs stabilized with different protective agents, since most experimental as well as theoretical work has been devoted to gold. In addition, recently, element-selective techniques such as XMCD and ^{197}Au Mössbauer spectroscopy have clearly demonstrated that ferromagnetic behaviour is intrinsic to the Au atoms that form the NPs [39, 77].

As XMCD analysis shows that the magnetic moment lies in the Au atoms, it can be inferred that this moment arises as a consequence of the bonding of the Au atoms at the NP surface with the capping molecules. The bonding may somehow modify the electronic structure of the Au surface. Therefore, the first objective is to reach a better understanding of the intrinsic details of the bonding.

Since Brust and co-workers reported a synthesis method for the preparation of gold nanocrystals passivated with covalently bound alkanethiols [78], an enormous effort has been made to functionalize these particles with alkanethiols or arenethiolates, as well as polymers [79], amines [42, 80], and different organic compounds. Some of these gold functionalized NPs have shown a new kind of magnetic order. Although bulk Au is diamagnetic, it was reported in 2004 that monodispersed Au NPs capped with dodecanethiol exhibited ferromagnetic-like behaviour even at RT [34, 37].

Bulk Au exhibits an electronic structure [Xe]$4f^{14}5d^{10}6s^1$ with negligible d–s hybridization and an fcc crystal structure. In contrast to Pd, Au is diamagnetic with a very low density of states at the Fermi level, $n(\varepsilon_F) = 0.29$ eV^{-1}/atom, low enough to promote noticeable Pauli paramagnetism [81]. Consequently, the weak 5d band paramagnetism is overcome by the combination of Landau and core diamagnetism and, as result, bulk gold is diamagnetic with a susceptibility of $\chi = -1.4 \times 10^7$ emu gOe^{-1} [82].

In 1999, Hori *et al* [73] reported unexpectedly large magnetic moments in Pd and Au NPs with particle sizes below 3 nm and embedded in poly(N-vinyl-2-pyrrolidone). Whereas the behaviour of Pd NPs was attributed to a size-dependent Stoner's enhancement, no explanation was given concerning Au NPs. By means of x-ray absorption near-edge structure (XANES) studies carried out at the Au $L_{3,2}$-edge, Zhang and Sham [83, 84] pointed out the influence of the capping system on the electronic structure of Au NPs. It was shown that Au atoms in NPs gain 5d electrons (relative to the bulk) when capped with weakly interacting dendrimers and lose 5d electrons when capped with strongly interacting thiol molecules. Thus, the d-electron distribution in the Au NPs can be tuned by selective capping.

In this way, dodecanethiol-capped Au NPs as well as Au NPs stabilized with a surfactant were synthesized by chemical routes [34]. This work reported the observation of magnetic hysteresis up to RT in gold NPs capped with dodecanethiol (CH_3–$(CH_2)_{11}$–SH). This behaviour contrasted with that exhibited by Au NPs with similar size but stabilized by means of the surfactant. In the latter, a diamagnetic behaviour similar to that of bulk Au was observed.

The thiol-derivatized gold NPs were prepared following essentially the Brust method [78], although the route was modified by increasing the thiol:gold ratio to decrease the average particle size. The second set of samples were tetraalkylammonium ($R_4N^+X^-$) protected gold NPs with a weakly interacting dipole capping molecule. Tetraoctyl ammonium bromide is the surfactant molecule and the particles were obtained following the Reetz method [74].

As an example, the magnetization curves of Au NPs capped with different thiol-containing molecules (Au–SR dodecanehiol and Au–SR maltose) are shown in figure 3. The magnetization corresponding to Au NPs stabilized with tetraoctyl ammonium bromide is also shown.

It should be noted that the hysteresis observed up to RT seems to indicate that the magnetic moments are blocked by high anisotropy. Since the blocking temperature may lie above 300 K this requires a value of the anisotropy constant, K, higher than 7×10^7 J m^{-3} or 10 meV/atom for this particle size. Such an enormous value could be reasonable on considering the high strength of the spin–orbit coupling for gold (1.5 eV) [85, 86].

Further information concerning the electronic structure of the NPs was obtained by combining XANES (x-ray absorption near-edge structure) with EXAFS (extended x-ray absorption fine structure) at the Au-L_3 edge. Of particular interest is the so-called white line that arises from the $2p_{3/2,1/2} \rightarrow 5d$ dipole transition, since the area under the white line gives information concerning the density of holes in the 5d band of Au [83, 84]. According to the area under the white line, charge transfer from gold to sulfur atoms is extremely large in the dodecanethiol-capped sample, as can be observed in figure 4.

Since gold NPs dispersed by a surfactant are diamagnetic, the ferromagnetic-like behaviour observed for thiol-capped Au NPs must be associated with the modification introduced in the Au electronic structure by the Au–S bond. This result indicates that the origin of the magnetic behaviour lies in the different interaction degrees between Au atoms and the protective molecule, and is in agreement with previous results published by Sham *et al* [84].

Another difference between both sets of samples is illustrated by means of surface plasmon resonance (SPR) measurements. Interaction of light with NPs could give information of the changes that occur in the electronic structure of the NP with decreasing particle size. SPR is one of the most remarkable optical properties of metallic NPs. The SPR is due to the collective oscillations of the electron gas inside the NPs that is correlated with the electromagnetic field of the incoming light, i.e., the excitation of the coherent oscillation of the conduction band. The excess of charge produced at the surface because of electron movement acts as a restoring force, while the electron movement is damped,

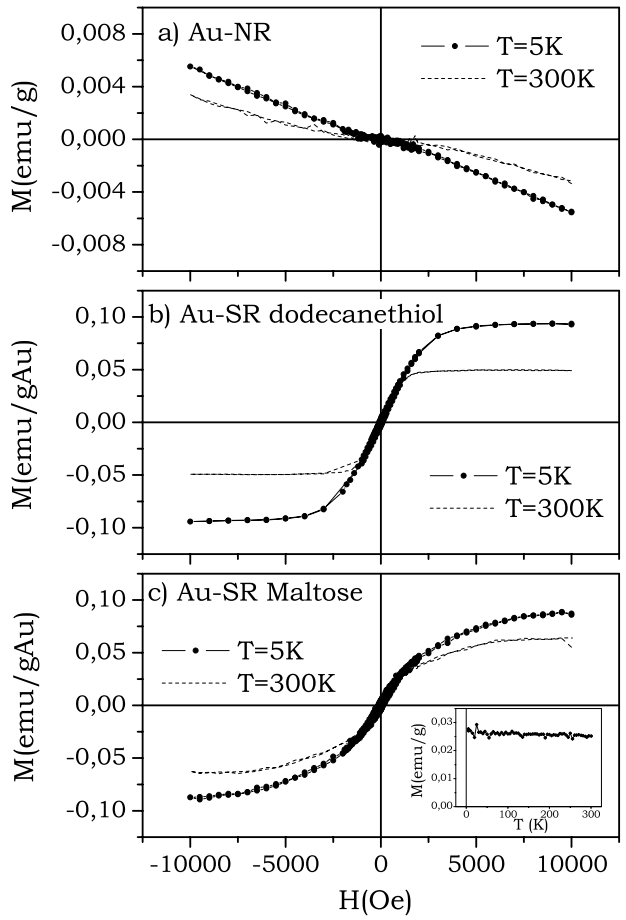

Figure 3. Magnetization curves of Au stabilized with different protective molecules: (a) Au-NR samples correspond to Au NPs stabilized by means of tetraoctyl ammonium bromide. TEM shows a bimodal particle size distribution centred at 1.5 and 5.0 nm; (b) Au–SR dodecanethiol, Au NPs with an average particle size of 2.0 nm capped with dodecanethiol; (c) Au–SR maltose, thiol-capped Au glyconanoparticles stabilized by maltose neoglycoconjugate and with an average particle size of 1.8 nm. The inset also shows the thermal dependence of the magnetization measured under an applied field of 500 Oe. ((a) and (b) reproduced with permission from [34]. Copyright 2004 American Physical Society. (c) reproduced with permission from [93]. Copyright 2006 American Physical Society.)

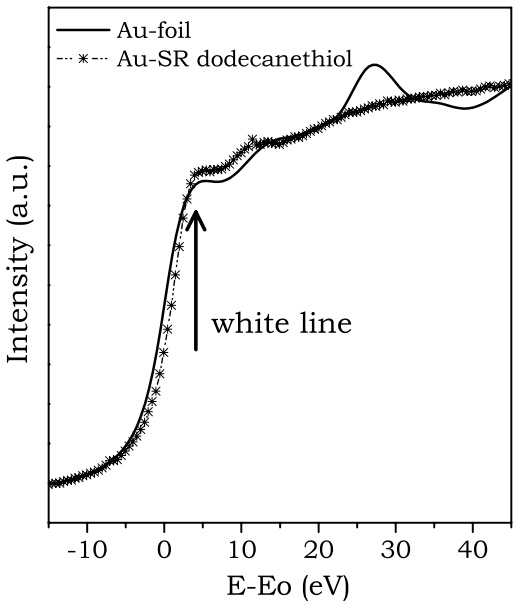

Figure 4. Au-L_3-edge XANES spectra for gold NPs compared to bulk gold.

mainly because of electron interactions with atomic cores and NP surface. The system behaves as a damped oscillator with a resonance frequency, which for most of the transition metals, lies in the ultraviolet–visible part of the spectrum. As the damping depends strongly on the particle size, the shape of the SPR also depends on the particle size. Therefore, the analysis of SPR gives information about the particle size and electronic configuration of the NP. The presence of SPR is a fingerprint for free electrons inside the NP (and, therefore, of its metallic character), while its absence indicates the localization of electrons. The SPR band is normally analysed within the framework of the Mie theory [87, 88]. As for capped Au NPs, García *et al* [89] have proposed a modified expression that takes into account that the region where electrons can oscillate freely is reduced by the chemical interface damping due to the Au–S bond. The thickness of the superficial layer depends on the intensity of the interaction between the capping agents and the Au atoms at the surface, i.e., the degree of localization of the electrical charges at the NP surface [35, 89]. In this work it was shown that the SPR is partially absent for thiol-capped samples, indicating that due to the Au–S bonding the 5d electrons of the gold NP have lost itinerancy and behave as localized or partially localized carriers, whereas the shape of the absorption curve for Au NPs stabilized with the surfactant is characteristic of isolated NPs without showing aggregation effects. The different shape of the SPR band for Au NPs with different stabilizing molecules is shown in figure 5.

Thus, the main conclusion that comes out of this work is that surface modification can deeply alter the magnetic properties of systems by changing the electronic structure of the NPs. Thiol bonding in Au NPs induces not only hole localization, but also permanent magnetic moments associated with the spin of extra d charge localized near the Au–S bonds. It was suggested that the strong spin–orbit coupling of Au, associated with high local anisotropy, freezes the magnetic moments along the local easy axis and gives rise to the appearance of permanent magnetism at the NP scale.

Guerrero *et al* [36] carried out a study trying to assess the influence of the metallic character of the NP on magnetic behaviour. Two sets of Au NPs functionalized with dodecanethiol with sizes of 2.0 and 2.2 nm were produced following the Brust method, although the Au:thiol ratio was modified to vary the particle size. Since this is a two-step method, an intermediate phase Au-thiol (polymeric) phase was isolated for study. The electron diffraction pattern of this sample showed the diffuse diffraction rings of an almost amorphous phase, i.e. no NPs were formed at this step of the reaction. Information about the electronic structure was obtained by means of XANES performed at the Au L_2-edge. The white line intensity corresponding to both sets of NPs decreased with respect to that of the polymeric

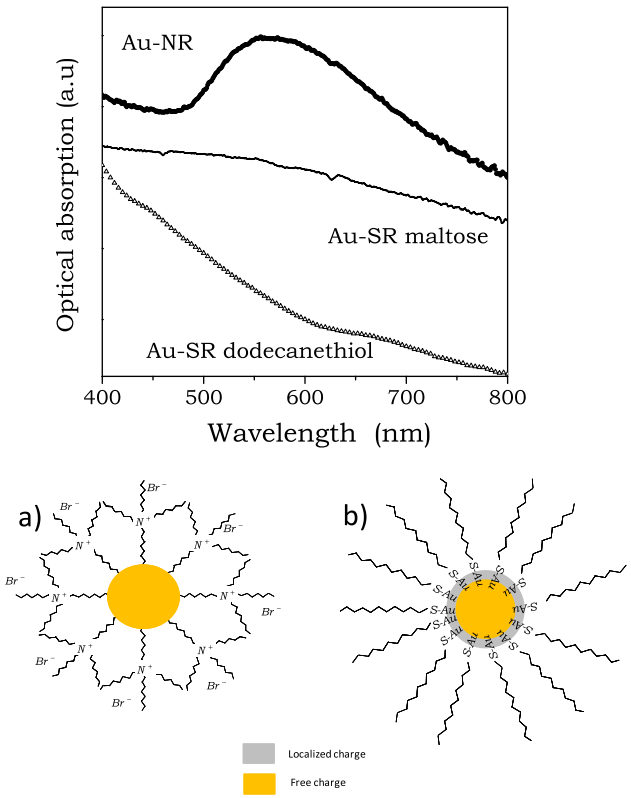

Figure 5. Upper panel: UV–visible absorption spectra for two sets of samples stabilized with thiol-containing molecules (Au–Sr dodecanethiol, Au–SR maltose). The spectrum of Au NPs stabilized by a surfactant (Au-NR) is also included (Reproduced with permission from [34, 93]. Copyright 2004 and 2006 American Physical Society.). Lower panel: (a) scheme of Au NP stabilized with weak interacting surfactant molecules, and (b) scheme of thiol-capped Au NP showing the external shell where electron movement is damped by interactions with thiols, and an inner metallic core where non-localized charges can oscillate.

sample. In addition, the Au-thiol (polymeric) sample showed Au–S distances and coordination numbers congruent with the formation of a –Au–S–Au–S– polymeric network and the absence of Au–Au metallic bonds. As regards the magnetic behaviour, both sets of NPs exhibited ferromagnetic-like behaviour, whereas the magnetization curve of the polymeric phase resembled that of a diamagnetic system. Thus, the presence of ferromagnetic-like behaviour is associated with the formation of NPs with the simultaneous presence of Au–Au and Au–S bonds.

The fact that not only Au–S bonds are required to observe ferromagnetism in capped Au NPs was also pointed out by Guerrero *et al* in 2008 [75]. In this study the magnetic behaviour of Au NPs capped with two different thiol-containing molecules but with different spatial configurations was compared, indicating that the way the chemisorbed molecules at the surface arrange is also a key factor. In this work, tiopronin-protected gold NPs were synthesized following the method developed by Templeton *et al* [90] and their magnetic behaviour was compared with that of dodecanethiol-capped Au NPs. Tiopronin is a thiol-containing biomolecule. Although Au–S bonds are present in dodecanethiol and tiopronin-capped Au NPs, the magnetic behaviour was quite different. In contrast to the ferromagnetic behaviour exhibited by thiol-capped Au NPs, the magnetization of the tiopronin-capped NPs exhibited a paramagnetic response at 5 K and at 300 K, which indicates that the magnetic moments induced through binding to S atoms fluctuate in orientation. In this case, the differences may arise from the geometry of the bonded molecules, since there are significant differences concerning their spatial arrangement possibilities: whereas dodecanethiol chains are well known to self-assemble [91], the self-organization of tiopronin is not a straightforward issue.

The dependence of the magnetic properties on particle size has been also studied. Dutta *et al* [77] reported the observation of a superparamagnetic blocking temperature of around 50 K in 5 nm diameter NPs but only diamagnetism was observed in 12 nm NPs. The samples under study were Au NPs capped with dodecanethiol. A magnetic moment 0.006 μ_B/Au atom was reported for 5 nm particles, which is attributed to holes in the 5d band of Au produced by charge transfer from Au to S atoms in dodecanethiol, as first suggested by Crespo *et al* [34]. The progressive loss of ferromagnetic-like character of thiol-capped Au NPs with increasing particle size has also been recently reported [40].

The presence of impurities is always a point to be considered. In most works, elemental chemical analyses have been carried out by means of inductively coupled plasma (ICP) analysis in order to estimate the amount of ferromagnetic impurities, essentially Fe. The level of ferromagnetic impurities found was, in all cases, too low to account for the magnetization values obtained.

Besides elemental analysis, some more specific studies have been conducted to elucidate whether the ferromagnetic-like behaviour observed in thiol-capped Au NPs is intrinsic to the NP. Au(Fe) glyconanoparticles (GNPs) with particle sizes below 2 nm were prepared by introducing a controlled amount of Fe impurities. The behaviour was compared to that of Au GNPs without Fe impurities. GNPs were prepared in aqueous solution by a one-step synthesis developed by Penadés *et al* [92, 93]. Thiol-capped AuFe and Au GNPs stabilized by maltose and lactose neoglycoconjugates with different Au:Fe ratios, as well as with different Au:S ratios, were studied by means of SQUID magnetometry and surface plasmon resonance [93]. The Fe content of the samples ranged between 0.06 wt% Fe and 2.8 wt% Fe.

In contrast to what was expected, spontaneous magnetization of AuFe GNPs exhibited a fast decrease with temperature that contrasted with the almost constant value of the magnetization observed in Au NPs, i.e. Fe-free NPs. Moreover, Au(Fe) NPs did not exhibit magnetic hysteresis at 300 K. In addition, SPR studies indicated that the absorption band became broader for the AuFe GNPs, whereas it was almost suppressed in the case of Au GNPs, indicating an increase of the damping of electrons due to charge localization at the surface promoted by the strong interaction between surface Au atoms and thiol capping molecules. Thus, the presence of Fe promotes delocalization with respect to Au GNPs.

The intrinsic magnetization of thiol-capped Au NPs was later confirmed by means of element-selective techniques

such as XMCD and Mössbauer spectroscopy [38, 39, 94]. These studies have clearly shown that the origin of ferromagnetic behaviour is not related to ferromagnetic impurities but it is intrinsic to the NP.

It should be mentioned that XMCD is a powerful technique allowing detection of magnetic moments of a particular element through sensitivity to the difference between the up- and downspin densities around the Fermi level. It is an element-selective technique that allows the evaluation of the magnetic signal originating from a particular element. XMCD is based on the fact that the absorption of light by matter may depend on the relative light polarization and the spin orientation of the atomic magnetic moments. Thus, when an electron has a certain polarization of the spin, the absorption of light at a certain edge will be different for right-handed polarized or left-handed polarized light. By measuring the absorption for both light polarizations, it is possible to calculate the magnetic moment of the electron by means of the so-called summation rules. Furthermore, the technique allows us to separate the spin and orbital contributions of the magnetic moment.

Garitaonandia *et al* [39] have combined XMCD measurements with ^{197}Au Mössbauer spectroscopy to determine the origin of magnetization in thiol-capped NPs. The NPs were prepared following the already mentioned Brust method. Their results demonstrated that magnetization in thiol-capped Au NPs is localized in the 5d orbital of Au atoms. Although the values of the magnetic moment per Au atom, 0.3 μ_B, were higher than those reported by others, the main conclusion of this study is that the gold atoms in the NP surface are carriers of the magnetic moment. Later, de la Venta *et al* [94] conducted a similar study on thiol-capped Au NPs embedded in polyethylene. Their results also showed that show that the magnetism observed in thiol-capped Au NPS is magnetism that is intrinsic to the NP and that cannot be attributed to para- or ferromagnetic impurities.

Ferromagnetism has not only been observed in Au NPs capped with thiol-derivatized molecules. Hori *et al* [43] have also reported ferromagnetic behaviour in Au NPs stabilized with polyacrylonitrile and poly(allylamine hydrochloride) (PAAHC). The ferromagnetic spin polarization of Au NPs protected by PAAHC with a mean diameter of 1.9 nm was measured by XMCD [37]. Au NPs coated with oleic acid and oleylamine with sizes below 7 nm and a narrow size distribution were also reported to exhibit ferromagnetic behaviour [42, 44]. High-resolution electron microscopy showed that the NPs exhibit fcc structure where multiple twinned planes are present. The calculated optical absorption spectrum is narrower than the experimental one, indicating that the oleic acid and oleylamine do not merely passivate the metallic NP but modify its electronic structure. The covalent bond of the organic molecules to the gold atoms of the surface induces ferromagnetic-like behaviour of the NPs similar to that of the thiol-capped counterparts, the features of which are an invariant temperature dependence of magnetization from 5 to 300 K and a noticeable coercive field.

More recently, ferromagnetic-like behaviour has also been observed in phosphine-capped Au NPs [41, 95]. It has been proved almost impossible to obtain subnanometer gold clusters using the Brust synthesis method. To obtain smaller Au clusters, Muñoz Marques *et al* [41] followed the method developed by Weare *et al* [96] to obtain small phosphine-stabilized Au NPs (diameter < 2 nm) and the procedures established by Bartlett *et al* [97] to obtain phosphine-capped undecagold clusters.

Two different types of gold nanomaterials were chemically synthesized: triphenylphosphine-capped undecagold clusters labelled as Au_{11}-TPP and with a composition estimated to be $Au_{11}(PPh_3)_7Cl_3$ and gold NPs with a composition of $Au_{225}(PPh_3)_{80}Cl_1$. Hysteresis loops showed ferromagnetic-like behaviour of the phosphine-stabilized gold NPs (nAu-TPP) whilst the phosphine-capped clusters (Au_{11}-TPP) did not present any magnetic features, being diamagnetic at low and high temperature. These preliminary results indicate that is possible to induce ferromagnetic behaviour by capping with ligands that do not contain a thiol group.

Theory and experiment have shown that the coverage of magic gold clusters by thiols of well-defined compositions is rather complicated [98, 99]. Sulfur atoms are attached with a single bond to a gold atom of the cluster [100, 101]. These magic or closed-shell clusters are highly ordered arrangements with full electronic sp shells, as in noble metal clusters in general [102]. Additionally, alkenethiols with longer chains on Au surfaces have been the focus of detailed theoretical studies [103] and the presence of several different metastable states are known. In these cases the sulfur atoms in the gold layers become arranged in a bridge configuration for the ground state.

The experimental findings in capped Au NPs are now supported by theoretical total energy calculations. Gonzalez *et al* [104], based on the results on thiol-capped Au NPs, presented a simple model that addresses the induction of magnetic behaviour in gold clusters on chemisorption of one organic molecule with different chemical linkers (nitrogen and sulfur linkers). The system under consideration was a small cluster of 13 gold atoms and one chemisorbed molecule. It was found that the interaction between S and Au orbitals was ultimately responsible for the onset of magnetism in thiol-capped gold nanoclusters, in agreement with the proposal of Crespo *et al* [34]. This model showed that, for a sulfur linker, energetic stabilization is accompanied by the development of spin localization preferentially in the gold atoms closest to the chemisorption site, whereas for a nitrogen linker, no spin symmetry-breaking leading to lower energy states is found. Later, different theoretical models have reported size-dependent magnetization and spin symmetry-breaking that would explain the experimental results found for thiol-capped gold and silver NPs [105–107].

Recent *ab initio* calculations show that the S–Au bond is such that an electron is transferred to the Au cluster. Therefore in the previous theoretical proposal the appearance of the magnetic moment in Au was always associated with either electrons or holes transferred from the capping molecules.

Thus, a second challenge is to account for RT ferromagnetism. In general the presence of hysteresis in

the magnetization curve of a sample indicates that the atomic magnetic moments are coupled to each other through exchange interactions. In fact hysteresis is due to magnetic anisotropy rather than to exchange interactions. In ferromagnetic NPs as small as 1.6 nm in diameter, the expected behaviour at RT is superparamagnetic, provided the usual values of anisotropy hold. For instance, Fe NPs are blocked if their diameters are larger than 30 nm. Then the question is: what is the strength and origin of giant anisotropy that forces a 6 nm diameter Fe (or Au) NP to remain blocked at RT?

Different proposals have been made. Vager *et al* [108] suggested that the applied magnetic field would induce a giant paramagnetic moment on those electrons involved in the bonding to the capping molecules.

The high magnetic anisotropy suggests that an orbital contribution to the magnetic moment cannot be disregarded. Hernando *et al* proposed a model that reasonably explains the orbital magnetism observed in different nanostructured films [109, 110]. This model [45, 46, 111] assumes the induction of orbital magnetism by motion of surface electrons around ordered arrays of Au–S bonds.

Thus, for the induction of an orbital magnetic moment, two requisites must be fulfilled. Firstly, it is necessary that the NP exhibits a metallic character (i.e. free electrons) and, secondly, Au–S regions at the surface exhibit some organization (i.e. the magnetic moment is proportional to the radius of the thiol-capped regions). It should be noted that at least a fraction of the surface electrons have to keep their mobility or delocalization in order to be available for being captured in the orbits.

This lacking accordance on the size and temperature dependence of the ferromagnetic behaviour is mainly due to the large dispersion of rather uncontrollable parameters which affect the onset of magnetism for these materials:

- *The relationship surface atoms to volume atoms*: the smaller this relationship is the more hindering the ferromagnetic-like behaviour is. This relation depends on particle size and, therefore, size dispersion has a huge influence on the onset of ferromagnetism. Small differences in size dispersion could induce different magnetic behaviour, favouring the occurrence of ferromagnetism as the monodispersion limit is reached.
- *The energy binding of organic molecules to surface atoms:* surface modification influences the magnetic properties of systems by changing the electronic structure of the NPs, and the thickness of the superficial layer depends on the intensity of the interaction between the capping agents and surface atoms [35, 36, 89]. The way the chemisorbed molecules at the surface arrange is also a key factor [75]. These factors are difficult to quantify.
- *The number of organic molecules bonded to the surface atoms*: the presence of ferromagnetic-like behaviour is associated with the formation of NPs with the simultaneous presence of Au–Au and Au–S bonds [36]; therefore, the real number of organic molecules bonded to the surface atoms play a key role and has not been yet precisely determined.
- *The experimental limit:* the very low magnetic signal of these materials forces the present experimental equipment to work at the resolution limits, hampering the distinction between the magnetic signal from the samples and any spurious signal from the experimental setup [112].

In summary, the existence of permanent magnetic behaviour in thiol-capped Au NPs has been well established by means of different experimental techniques, including element-selective techniques (XMCD and Mössbauer spectroscopy), showing that the observed behaviour is intrinsic to the NP. The phenomenon, however, is far from being well understood.

3.2. Magnetic properties of ZnO NPs

The potential applications of magnetic semiconductors in spintronics have motivated the research work of a large number of groups around the world [113–118]. The main objective was concentrated on diluted magnetic semiconductors (DMS), consisting of a semiconductor matrix in which some small fraction of ferromagnetic impurities is embedded [119, 120]. After obtaining some promising results using ZnO [115] as the host semiconductor, some controversy marked the subsequent discussion on the origin of the magnetization [121], as we will overview in section 3.3. A large number of theoretical as well as experimental results are available in the literature of nitride and oxide semiconductors, with conflicting results on RT ferromagnetism [122–124].

On the basis of quantum confinement effects there is also a tremendous interest in the behaviour of oxide and semiconductor NPs. Ferromagnetism at RT in some oxide NPs such as CeO_2, Al_2O_3, ZnO, In_2O_3 and SnO_2 has been reported. These observations lead to the conclusion of the universal character of ferromagnetic behaviour in oxide NPs [125, 126].

It was shown [32, 127] that Mn:ZnO NPs exhibit RT ferromagnetism when capped with molecules that introduce p-type defects, while when capped with molecules that introduce n-type defects, no RT ferromagnetism is observed. By contrast, for CoZnO films, n-type defects favour the appearance of RT ferromagnetism whereas p-type defects do not result in RT ferromagnetism. These experiments indicated the importance of the electronic structure of the semiconductor (modified by the presence of the magnetic impurities and defects) in the appearance of the observed magnetism. To ascertain the relative influence of both magnetic impurities and defects in the appearance of ferromagnetism, a study on ZnO NPs capped with different molecules was carried out. In this case ferromagnetic impurities were not introduced. García *et al* [32] prepared ZnO NPs by the sol–gel method and subsequently capped with three different organic molecules: tryoctylphosphine (TOPO), dodecylamine (AMINE) and dodecanethiol (THIOL), which bind to the particle surface through O, N and S atoms respectively. X-ray diffraction and transmission electron microscopy indicated for all three cases the formation of hexagonal ZnO NPs (wurtzite structural type) with average

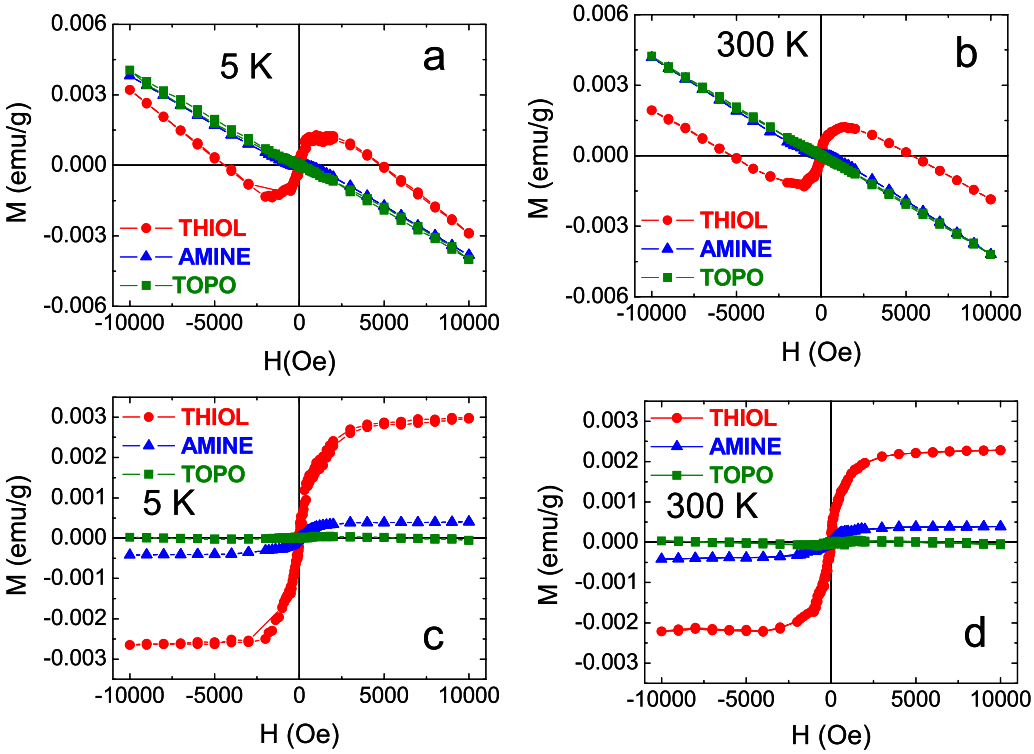

Figure 6. (a), (b) Experimental hysteresis loops from ZnO NPs capped with different molecules. (c), (d) The loops after subtracting the diamagnetic/paramagnetic background. (Reproduced with permission from [32]. Copyright 2007 American Chemical Society.)

particle sizes of around 10 nm. High-resolution electron microscopy confirmed the hexagonal structure. No differences in structure were observed in the NPs. However, the XANES spectra at the Zn–K-edge measured at RT were clearly different for the three cappings. The Zn–K-edge corresponding to the 1s → 4p Zn transition was found to be more sensitive to the Zn chemical bonding than the L edges. The intensity of the first maximum of the XANES spectra was associated with the amount of charge transfer between the Zn atoms and the surrounding atoms. Photoluminescence (PL) spectra of the three types of ZnO NPs also showed a remarkable dependence of the PL visible emission on the type of capping molecule: 2.3 eV emission (corresponding to photons with 550 nm wavelength) is clearly observed for the TOPO sample, being weaker for the AMINE sample and absent in the spectrum for the THIOL sample (see figure 3(b) [32]). This is in agreement with a surface origin of this effect, as the molecules can alter only the surface electronic structure. These results can be understood by assuming that the binding energy associated with a type of molecule controls the number of deep-level recombination centres or that it induces new surface states that provide alternative decay paths, hence, quenching the PL emission. These differences in both XANES and PL spectra indicate differences in the electronic structure of the NPs despite their identical atomic distribution structure observed by x-ray diffraction and electron microscopy.

The magnetization curves shown in figure 6 indicate that, besides the diamagnetic signal characteristic of bulk ZnO, a ferromagnetic component appears for the NPs capped with

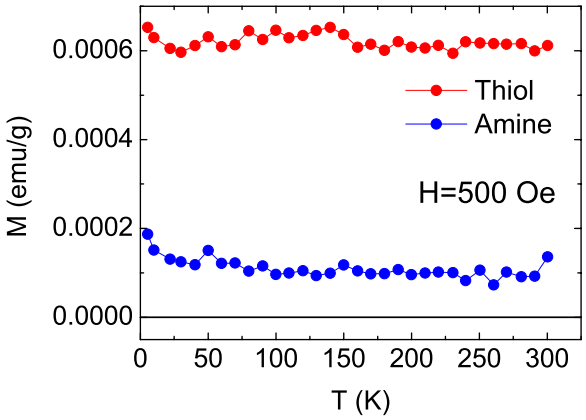

Figure 7. Magnetization versus temperature for ZnO NPs capped with thiol and amine under an applied field of 500 Oe. The corresponding constant diamagnetic background has been subtracted. (Reproduced with permission from [32]. Copyright 2007 American Chemical Society.)

amine and thiol. The ferromagnetic component became more evident when the diamagnetic contribution was subtracted, as also illustrated in figure 5. For both cases the average sizes of the NPs were 10 nm and the magnetic moments per surface atom, obtained from the saturation value, were 2×10^{-3} μ_B and 0.5×10^{-3} μ_B for thiol and amine samples respectively. A remarkable point is the constant value of the magnetization in the range 5–300 K, as shown in figure 7. These characteristics of magnetic behaviour are very similar to those found for functionalized Au NPs, as discussed in section 3.1, and for

the NPs of different oxides as reported by Sunderasan [126] and other authors [128].

The perfect correlation in the evolution of the electronic structure, modified by the capping molecule, with the magnetic response of the sample is worth noting. Those NPs showing the highest XANES absorption (thiol) also exhibit the highest magnetic moment.

Two conclusions, as indicated in Nature Materials Highlights [129], were derived from this study: (a) a magnetic moment is induced in ZnO independently of the presence of ferromagnetic impurities and (b) this component comes from the modification of the electronic structure induced by the capping molecules.

The similarity of magnetization dependence on both field and temperature as well as in the value of the magnetic moment per atom between the capped ZnO and Au NPs suggest that such magnetism should originate at the surface of the NPs when subject to different modifications of their electronic configuration.

Deeper experimental studies on the magnetism of ZnO NPs, capped with the same molecules as in the previous García *et al* article [32], were later performed by Chaboy and others [130, 131]. XMCD was used to analyse the origin of the magnetism, leading to the conclusion that this exotic magnetism arises at the hybridized band formed between Zn and the bonding atom of the molecules. The formation of a well-defined interface between ZnO and the capping molecule was observed. Therefore, two different types of Zn atoms can be distinguished. It is obvious that the magnetism is not induced in the 3d band of Zn, because in the measured energy region no XMCD signal could be observed. By contrast, a clear XMCD signal is found at the Zn–K-edge. This result indicates that the magnetization is intrinsic and, furthermore, that it relies on the 4sp Zn conduction band. This finding represented a break from the commonly accepted point of view that the 3d band plays an important role in the magnetism of semiconductor oxides.

Ferromagnetic-like behaviour at RT was also observed in other semiconductor NPs such as CdSe:Cu and thiol-capped CdSe [129]. Sundaresan *et al* [126] reported the ferromagnetic character of CeO_2, Al_2O_3, ZnO, In_2O_3 and SnO_2 at RT in 2006. More recently, Taylor *et al* reported a hyperfine magnetic field of around 11 T at RT in HfO_2 and ZrO_2 NPs measured by the ^{181}Ta perturbed angular correlation technique for particle sizes lower than 5 nm [132–134].

Magnetism in oxide NPs, as in any other type of NPs formed by substances that are not magnetic in bulk, presents several common features, such as a low dependence on the temperature, a low saturating field (around 0.5 T), a magnetic moment of the order of 10^{-2} μ_B/atom, a low coercive field and low remnant magnetization. Due to the low magnetization values, special care must be taken to estimate the possible influence of magnetic impurities [112]. It can be concluded that the analysis performed by XMCD is the only definitive test to ensure the intrinsic character of the magnetization measured macroscopically.

3.3. Efforts in understanding anomalous magnetism of NPs

Observations of ferromagnetic behaviour in NPs made of substances that are not magnetic in bulk clearly indicated that a nanoscale intrinsic source of magnetization is present. From the previous overview of the experimental results it can be concluded that this component of the magnetization of NPs seems to be universally induced at the surface. As experimentally found using XMCD, modification in the surface electronic structure results in modifications of the surface magnetic properties. Note, however, that in ferromagnetic NPs the surface component of the magnetization is masked by the core contribution. A characteristic of this surface component is that it is almost independent of temperature up to RT and that it saturates at relatively small fields of around 0.5 T. It is also obvious that the relative importance of this surface component should decrease with increasing NP size. Therefore, independently of the effects that have been customarily used to account for ferromagnetism in metals and diluted magnetic semiconductors, there may be a characteristic surface physics effect underlying the surface magnetization of NPs. For instance, surface magnetism in oxide NPs may only be partially explained in the framework of the well-known models proposed to account for magnetism in diluted magnetic oxide and semiconductors [115, 121–124]. It should be indicated that the origin of the magnetism observed in bulk semiconductors, doped with either magnetic or non-magnetic atoms, and even undoped, is far from being well understood.

As concerns the experimental values of the magnetization in NPs, it must be remarked that a large variation in the reported values of the saturation magnetization appears in different articles. The influence of the capping coverage factor, the nature of the capping molecule and the size of the NPs might explain these differences. However, the contribution of magnetic atoms diluted as non-detectable impurities together with the low values of intrinsic magnetization must also be considered as a tremendous drawback to the accuracy of the magnetization measurements. In an interesting article, Sundaresan and Rao [135] have invoked the universality of ferromagnetism in inorganic NPs. They propose that the observed ferromagnetism is a surface effect due to the presence of defects. As is known, point defects in insulators can create localized electronic states within the band gap with different electron occupancies and different electric charge and magnetic moments. A short-range ferromagnetic interaction with a correlation length of four neighbours have been shown to allow ferromagnetic percolation for 4.9% of vacancies in CaO [136]. Consequently, the surface component of the magnetization in NPs may then originate from short-range exchange interactions acting among the magnetic moments induced at surface point defects.

In particular, TiO_2 magnetism has been extensively studied for bulk and nanostructured samples for a long time [137–139]. Ferromagnetism of TiO_2 thin films, without the introduction of ferromagnetic impurities, could be neatly

explained by a double exchange mechanism [137]. However, Coey *et al* [140] have revisited the magnetism of oxide NPs and focused on TiO_2 (rutile). They proposed a new theory that corrected the first impurity band model that included effective Heisenberg exchange interaction between 3d local moments within magnetic polarons [141]. In this new theory they invoke inhomogeneous Stoner-type ferromagnetism associated with percolating defect structures. Charge transfer to or from a charge reservoir into a narrow band, associated with defects, can induce inhomogeneous Stoner-type wandering axis magnetism.

An important theoretical analysis was based on the observation that in low-dimensional ZnO, RT ferromagnetism appears for non-magnetic doping and even for undoped samples. This analysis carried out by Sánchez *et al* [142] showed that the spin polarization of the polar (0001) oriented surfaces of wurtzite ZnO was enhanced even in the absence of magnetic ions.

Even though many different contributions have been reasonably invoked, it seems clear that a characteristic contribution comes from the nanoscale as regards the magnetism of NPs. The similarity observed between the magnetic behaviour of very different types of NPs, such as functionalized Au and ZnO, strongly suggests that a common source of magnetization may be contributing in any NP.

In recent publications, Hernando *et al* [49, 143] have shown that large orbital magnetic moments can be found in the framework of the quasi-free electron approximation for the electrons of the surface band of NPs. Electrons forming a two-dimensional gas on a spherical surface of nanometre radius behave in a way that is intermediate between atoms and solids. They showed that, depending on the NPs radius, NPs can behave as atomic systems for sufficiently small radius.

The eigenstates of free electrons confined on a spherical surface, such as those donated by the capping molecules or any impurity, are spherical harmonics instead of being plane waves. Free electron eigenstates are kinetic energy eigenstates. The spherical symmetry gives rise to free electron wavefunctions characterized by the angular momentum, l, and quantum number [144].

If the number of electrons confined on the NP surface is N_b, it can be seen that they distribute over the energy spectrum to reach a Fermi level, l_F, given approximately by the square root of N_b. According to the Hund rules, the electrons occupy successively different states of their Fermi level, reaching the maximum spin and the maximum orbital momentum compatible with the maximum spin condition. In an assembly of NPs, due to radius and N_b fluctuations, there should be a uniform distribution of the occupation number of the Fermi level as well as a distribution of the Fermi level itself. It is straightforward to see that for a constant Fermi level and a uniform distribution of its occupancy, the average magnetic moment associated with NPs for which their Fermi level is unfilled is given by the square of l_F times the Bohr magneton. Therefore, the spontaneous magnetic moment of the surface band of an assembly of NPs for which the average Fermi level corresponds to $l_F = 20$ becomes of the order of 400 Bohr magnetons. The Zeeman splitting, for a 1 T applied field, should be of the order of 5×10^{-2} eV, twice the thermal energy at RT. These considerations explain the main characteristics of the experimental magnetization observed in NPs.

The strength of the paramagnetism is expected to be giant, since an applied magnetic field of 1 T would induce a maximum Zeeman splitting of $2\ \mu_B l_F^2$ that is larger than the thermal energy at RT for any $l_F > 10$. It can be concluded that the Langevin or Brillouin curves depicting the paramagnetism of NPs is close to saturation, i.e., $\mu_B(\frac{1}{3}l_F^2)B/k_BT \geq 1$, for $B = 1.5$ T and $T = 300$ K if l_F is larger than 10, which is a very reasonable value for the size of the NPs experimentally studied.

It can be concluded that the anomalous magnetism observed in NPs that are not magnetic in bulk has its source at the NP surface, and its contribution decreases relatively to that of the bulk as the size of the NPs increase. Its strength can be modified by tuning the electronic and atomistic structure of the surface. Its intrinsic origin is not well understood. However, the use of selective techniques, such as Mossbauer and XMCD, has neatly indicated that the magnetism is intrinsic to the NP atoms and not only due to possible magnetic impurities.

4. Biocompatible coatings on ferromagnetic NPs

The use of magnetic NPs for biomedical applications requires NPs without toxic or injurious effects on biological systems. Due to synthesis procedure or atomic composition, most of the as-synthesized particles are non-biocompatible; therefore, it is necessary to coat them with a biocompatible organic or inorganic shell. Sometimes, the coating merely gives colloidal stability, but sometimes it can drastically affect the NPs magnetic properties.

4.1. Inorganic coatings on ferromagnetic NPs

Surface modification of nanometre ferromagnetic cores with different inorganic shell-like metals or oxides to form core/shell-type nanostructures has become an important route to producing multifunctional nanomaterials. Such modifications bring about interesting physical and chemical properties of nanostructured materials that have important technological applications.

4.1.1. The metallic coatings. The interest in gold-coated ferromagnetic NPs lies in their potential biological applications. The gold coating allows easy conjugation of DNA, proteins and diverse biomolecules [145, 146]. Since gold is a conducting metal, the gold coating allows inductive heating by applying an alternating magnetic field (AMF) and the heating power can be increased by hysteresis losses in ferromagnetic materials, thus resulting in promising materials for hyperthermia treatments. However, the coating does not merely act as a barrier protecting the NPs against external agents; it also modifies the material structure and plays a fundamental role in the interface coupling interactions [54, 147].

Equiatomic FePt has a high Curie temperature, large magnetic moment and magneto-crystalline anisotropy and

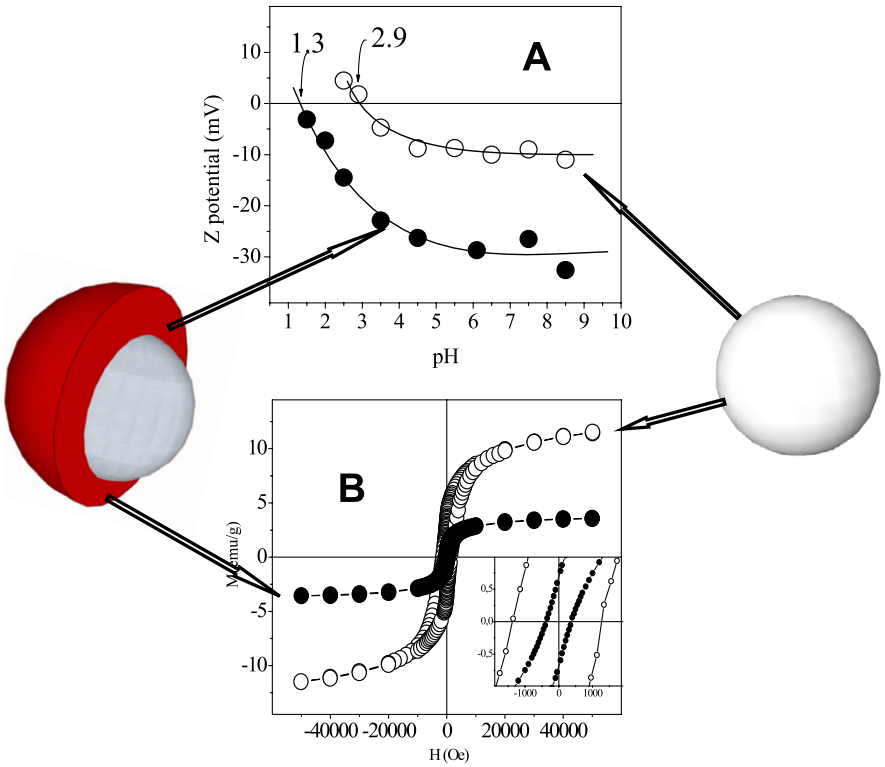

Figure 8. (A) *Z* potential of the MUA ligand-exchanged FePt (open circles) and FePt@Au (full circles) NPs. (B) Magnetization curves of FePt (open circles) and FePt/Au core–shell (full circles) at 5 K. The inset shows the change in the coercive field. (Reproduced with permission from [61, 149]. Copyright 2008 IEEE and copyright 2008 American Institute of Physics.)

excellent chemical stability. Despite the effort to synthesize small monodisperse FePt NPs in the hard phase, most of the synthesis methods produce FePt NPs in the disordered fcc phase, i.e., a soft material which is ideal for biomedical applications [51, 145, 146, 148]. Besides, several authors have reported that small FePt NPs are subject to corrosion due to the inhomogeneous concentration of Fe atoms, which is higher at the NP surface [148–150]. By protecting the FePt NPs with a gold shell it is possible to prevent the NPs from oxidation in addition to taking advantage of coatings that can be widely functionalized, making the FePt-based core–shell nanostructures excellent candidates for biological applications [151].

When ferromagnetic NPs are coated by Au [50, 51, 53], the magnetic properties are affected not only by the presence of a diamagnetic compound but also because the gold atoms interact at the interface with the core atoms. De la Presa *et al* [50] reported that both the FePt and FePt@Au NPs are superparamagnetic at RT, and the saturation magnetization M_s, coercive field H_c and blocking temperature T_B are reduced due to the presence of a few nanometres of diamagnetic gold shell (see figure 8(B)). Similarly, Yano *et al* [51] showed that the FePt and FePt@Au NPs synthesized in this way have a disordered fcc structure and are superparamagnetic at RT. Since T_B and H_c are related to magnetic anisotropy, and assuming the bare FePt NPs are monodomain, then T_B is proportional to the anisotropy energy $T_B = KV/25\ k_B$ and, below T_B, H_c can be approximated by $H_c \approx 2\ K/M_s$ [152–154]. Therefore, the decrease of coercive field and blocking temperature reflect the decrease in magnetic anisotropy. Although the interaction between FePt and Au atoms at the interface is not well understood, these results suggest that the presence of the gold atoms leads to a reduction in surface anisotropy [50].

De la Presa *et al* [61] showed that FePt@Au NPs which have oleic acid and oleylamine as surfactants and are dispersed in hexane, can be ligand-exchanged to mercaptoundecanoic acid to get water-stable FePt@Au NPs (see figure 8(A)), without affecting the magnetic properties of the original NPs. On the other hand, Hartling *et al* reported [53] that a thin gold layer formed on the FePt NPs strongly increases the stability of their magnetization under ambient conditions in the long term: the gold coated NPs still showed magnetic contrast after for four months ageing, while the naked FePt NPs lost their magnetic properties completely [149]. Gold coatings can also prevent the NPs from sintering when thermal annealing at high temperature is performed: FePt@Au NPs partially transform from a disordered fcc phase to an ordered $L1_0$ phase, which has stronger magnetic anisotropy [51].

Whereas gold coating prevents the ferromagnetic metallic cores from oxidation, the coating of iron oxide by gold brings the possibility of producing very efficient nanostructures. The influence of a gold shell on gold coated superparamagnetic iron oxide NPs (Fe_3O_4@Au) has been investigated by several authors [145, 155–161]. Wang *et al* [155] reported that

Fe_3O_4@Au NPs retain superparamagnetic behaviour at RT; however, T_B and H_c are reduced after gold coating, reflecting the decreased coupling of the magnetic moments as a result of the increased inter-particle spacing of the magnetic cores. Their findings are also supported by other authors [145, 159–161].

On the other hand, an enhancement of the magnetic moments in Fe_3O_4@Au NPs has been recently reported, in which large magnetic cores of about 100 nm size are coated with a thick gold shell of 50 nm thickness [156–158]. Banerjee *et al* [157] attribute this effect to the chemical potential gradient at the interface of the Fe_3O_4@Au, which could be enough to trap the conduction electrons from the Au particle, inducing a large orbital moment at the interface, similarly to thiol-capped Au NPs [34]. Therefore, the increase in magnetic moments would come from the metallic electrons at the Au–Fe_3O_4 interface, with the moment being predominantly orbital. A large interface in the core–shell NPs is necessary to cause an increase in net magnetic moments.

To summarize, gold coatings provide not only a versatile cover for functionalization with different biomolecules but also modify the magnetic properties by isolating the magnetic cores or by the interaction of the interface atoms.

4.1.2. Oxide coatings. Most important requirements for biomedical applications can be achieved by core–shell NPs with a controllable thickness of biocompatible silica shell in the form of completely non-aggregated, single-core nanocomposites and stable suspension [162].

Silica coatings also offer a platform to obtain thermally stabilized FePt NPs in the hard magnetic phase. The silica coat can prevent sintering when NPs are subject to thermal annealing and make the FePt NPs behave as non-interacting single domains due to the increase in the inter-particle spacing. Even though the sizes of the NPs can be below 10 nm (well below the critical size) and the silica coat thickness can vary from 5 to 25 nm, they are able to totally or partially transform from the disordered fcc soft to the $L1_0$ hard magnetic phase and can therefore be permanently magnetized at RT [163–165]. Different parameters must be considering for getting the FePt@SiO_2 NPs to transform to the hard phase: (i) the thermal temperature must be higher than 700 °C, (ii) a reducing atmosphere is required and (iii) the silica thickness also plays a role in the phase transformation [163–165].

The silica coatings are another way of protecting NPs against corrosion. Aslam *et al* [166] were the first to coat FePt NPs with silica, stabilizing the metallic NPs and making them water dispersible after silica functionalization. The magnetization behaviour of silica coated FePt NPs indicates a diamagnetic contribution from the shell to the net magnetization of the FePt NPs. In addition, a convenient and efficient method of reversible phase transfer of ferromagnetic silica coated L1(0)-FePt NPs from aqueous to organic phases was developed by Yamamoto *et al* [167], in which the magnetic properties remained unaltered. Chen *et al* [162] also reported the advantages of synthesized FePt@SiO_2 NPs for *in vivo* imaging applications, although the NPs have reduced magnetic saturation and lower relaxivity parameter compared to the uncoated FePt NPs. However, biocompatibility studies showed the absence of cytotoxicity during seven days at concentrations below 30 μg ml^{-1}, which was attributed to the strong surface coating. In addition, 7 T magnetic resonance imaging (MRI) studies showed that both FePt and FePt@SiO_2 NPs are strong T_2 contrast agents, which in addition to the high degree of biocompatibility makes FePt@SiO_2 NPs an ideal platform for the design of diagnostic and therapeutic agents as MRI contrast agents or hyperthermia treatments.

The silica coating of iron oxides can improve the water stability since this kind of surface provides additional steric repulsion. Furthermore, it can be easily functionalized with active groups such as amine, carboxyl, aldehyde and thiol groups. Gonzalez-Fernandez *et al* [168] produced highly stable Fe_3O_4@SiO_2 core–shell NPs with magnetic core sizes ranging from 20 to 50 nm. The control of the ferromagnetic core size allows fitting the size around 30 nm to reach the maximum specific absorption rate (SAR) for hyperthermia application. The specific absorption drops rapidly for sizes that differ from this value by a few nanometres. The silica coating decreases the isoelectric point to a half, from pH = 5–2.5, making the Fe_3O_4@SiO_2 water stable in a wider pH range than uncoated NPs (see figure 3 from [168]). However, the SiO_2 coating plays a significant role in the SAR mechanism by hindering the heat flow, thus decreasing the heating efficiency. A compromise must be made between the surface functionality and the heating efficiency, probably making the shell thickness as thin as possible.

Vogt *et al* [169] synthesized Fe_3O_4@SiO_2 core–shell structures for biomedical applications. The silica shell thickness ranged from 5 to 13 nm thick and the Fe_3O_4@SiO_2 showed a superparamagnetic character with high magnetization, rendering the material useful for biological applications. The drawback lies in the limited amount of material that can be synthesized in one batch; however, for biomedical applications such as drug delivery systems, MRI contrast agents, cell separation, etc, small amounts of high-quality samples are required.

The treatment of tumours by hyperthermia is based on the fact that there exist a temperature window at which tumour cells are more susceptible to heat than normal ones [13]. By taking advantage of this temperature window, it is possible to kill tumours selectively by applying an AMF to a magnetic colloid in a tumour, thus inducing a selective heating. However, if the temperatures exceed 60 °C, serious damage can be caused on the normal tissues as well as risk an increase of severe or persistent side effects. To overcome the obstacle of temperature control, new materials of tunable Curie temperature (T_c) are being intensively investigated [52, 170–174]. The new materials must satisfy strict conditions such as biocompatibility (nontoxicity), stability in aqueous solution and possess high thermal efficiency as heating elements. Magnetic particles with tunable T_c will prevent the temperature of the whole tumour or the hottest spots around the particle rising over T_c, avoiding the use of any local temperature control system.

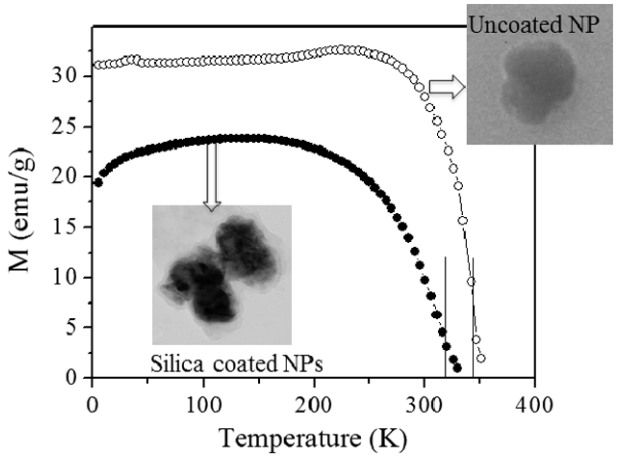

Figure 9. Magnetization curves versus temperature for $La_{0.56}(CaSr)_{0.22}MnO_3$, as prepared (open circles) and silica coated NPs (full circles). The vertical lines indicate the Curie temperature for both silica coated ($T_c = 317$ K) and uncoated NPs ($T_c = 341$ K). (Reproduced with permission from [52]. Copyright 2010 American Chemical Society.)

In complex cationic compositions such as $La_xSr_{1-x}MnO_3$ it is possible to have fine control of T_c; however, the Sr and La content can be toxic for *in vivo* experiments. Water stability at high concentrations and biocompatibility are achieved by coating the magnetic manganese oxide NPs with 10 nm thick silica. However, the silica coat significantly affects the magnetic properties: (i) T_c decreases and (ii) the total magnetization is reduced by the presence of diamagnetic silica [52, 171].

Villanueva *et al* [52] reported that, at RT, magnetization at 1 kOe is decreased by about 32% for the coated particles. The large amount of diamagnetic silica can account for the decrease in the total magnetization values. This reduction in magnetization is expected to reduce the heating efficiency of the material, as has been observed for iron oxide NPs [168].

On the other hand, T_c reduction is better related to the interaction of silica with atoms at a manganese oxide surface. The presence of silica reduces T_c by only 7%, from 341 K (68 °C) to 317 K (44 °C) (figure 9). However, considering the narrow temperature range at which hyperthermia treatments are performed, the decrease from 68 to 44 °C is relevant.

The application of an AMF of 15 mT and 100 kHz for 30 min to HeLa cells after incubation with silica coated manganese oxide NPs induced cellular damage that finally led to apoptotic cell death even though the temperature increase in the cell culture was lower than 0.5 °C (see figure 10) [52]. Recently, *in vitro* studies in magnetic NP loaded dendritic cells have demonstrated also the feasibility of inducing dramatic cell death without increasing the macroscopic temperature during AMF exposure [175]. These results indicate that local effects (such as local heating or morphological cell damage) are relevant for the apoptotic cell mechanism and that the heat is not the only agent responsible for triggering cell death following hyperthermia treatment.

Therefore, a compromise needs to be achieved for the silica coating, which should be thick enough to assure water stability at high NP concentrations while keeping the magnetization as high as possible to preserve the heating efficiency.

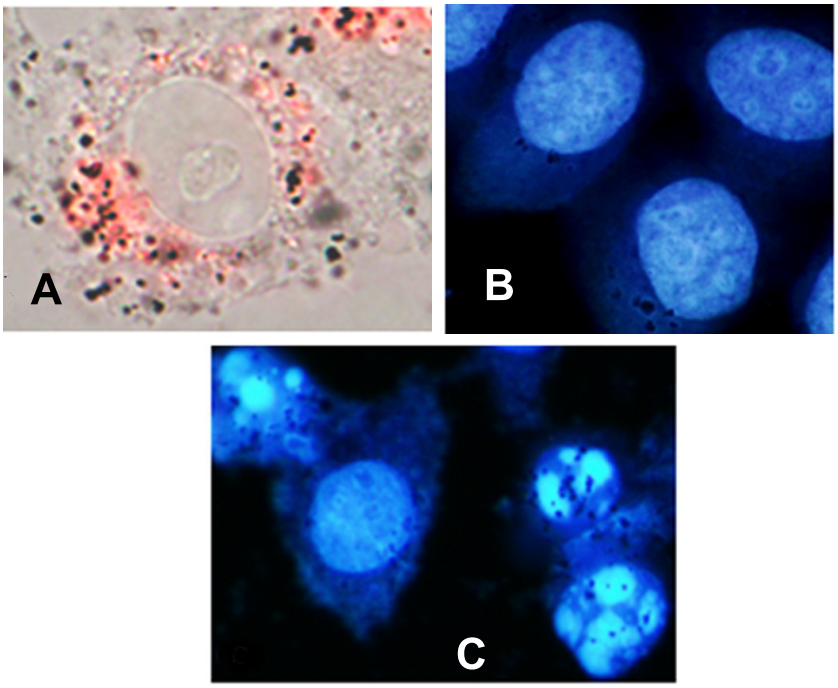

Figure 10. (A) HeLa cells incubated with 0.5 mg ml^{-1} silica coated manganese oxide for 3 h observed in bright-field microscopy and fluorescence overlay. (B) Interphase cells treated only with silica coated manganese oxide and stained with Hoechst-33258. (C) Morphological changes of attached HeLa cells induced by applying an AMF 24 h after treatment. (Reproduced with permission from [52]. Copyright 2010 American Chemical Society.)

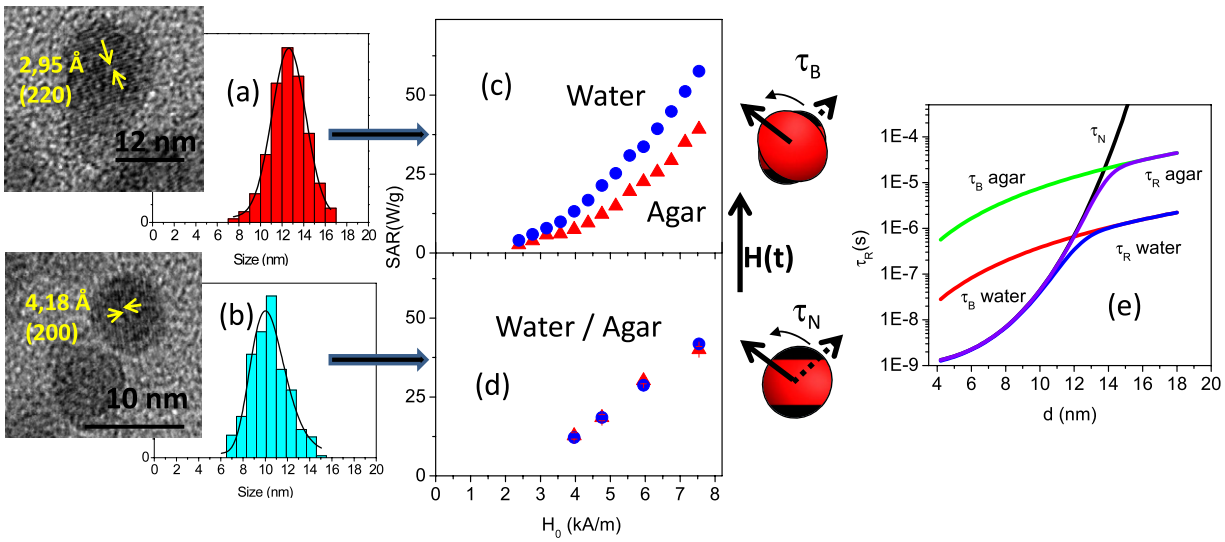

Figure 11. (a), (b) HR-TEM images and size distribution for 11 and 14 nm γ-Fe_2O_3 NPs. (c), (d) SAR values as a function of field amplitude for γ-Fe_2O_3 NPs dispersed in water (blue circles) and agar (red triangles); the SAR of the smaller NPs is independent of the carrier viscosity indicating that the relaxation mechanism is mainly due to Neel relaxation. (e) Neel–Brownian relaxation times τ_R as a function of size for water and agar carriers. (Reproduced with permission from [59]. Copyright 2012 American Chemical Society.)

4.2. Biocompatible organic coatings: the effect of aggregates on the magnetic properties

The investigations on the heating efficiency of magnetic NPs under an AMF for tumour hyperthermia applications have increased exponentially in recent years [52, 176–181]. The present challenge is to find biocompatible magnetic NPs with high SAR values that can be synthesized in large quantities in an easy, cheap and reproducible procedure, looking for the assessment of the scalability limits of the treatment. In the frame of the linear response theory, SAR varies as the square of field amplitude H_0 and linearly with the frequency f of the AMF. However, more systematic studies as a function of particle size, coating and concentration are highly desirable in order to yield progress in the prediction and optimization of the heating efficiency of magnetic NPs under an AMF for applications in magnetic hyperthermia [182].

The heating efficiency is expected to be influenced by any parameter affecting the magnetic interactions between particles and therefore the magnetic moment rotation. In fact, magnetic interactions have been observed to significantly diminish the dipolar magnetic field outside a capsule when particles are highly packed [58]. In the same sense, SAR has been observed to increase with magnetic NPs size up to a certain value [183], but the dependence of this parameter with the viscosity of the medium is not so clear [178, 184–186]. The NPs shape is another parameter to be considered in the optimization of the heating efficiency. For example, ferromagnetic nanocubes seem to exhibit superior magnetic heating efficiency compared to spherical particles of similar sizes [181, 187]. The cubic shape resembles magnetostatic bacteria, and the beneficial role of surface anisotropy could be recognized as an important mechanism for the development of magnetic hyperthermia for cancer treatment.

Recently, de la Presa *et al* [59] showed that surface modification by aminopropylsilane (APS) coating of γ-Fe_2O_3 does not affect the NPs heating efficiency, making these NPs good candidates for hyperthermia treatment as well as model samples for the standardization of hyperthermia apparatus. The NPs synthesized by the co-precipitation method, with sizes ranging from 6 to 14 nm, showed low polydispersity (0.2) and a high degree of crystallinity [188]. Neel–Brown relaxation times about 10^{-7} s are obtained from the SAR field frequency dependence (figure 11). However, if the particles are immobilized in agar, the larger particles became less effective than the smaller ones due to the viscosity increase.

In summary, organic coatings which improve the colloidal properties and sample biocompatibility could have a bearing on the heating efficiency since magnetic properties can be altered by the formation of the chemical bonds at the NP surface or the formation of different aggregates. The organic coating can also affect the Brownian relaxation time due to its dependence on hydrodynamic size.

Magnetic NPs are also interesting contrast agents for MRI thanks to their ability to affect the relaxation rate of water protons, causing a decrease in signal intensity that results in a darkening effect in the corresponding MR image [189]. Particles synthesized by different procedures exhibit differences in their physicochemical characteristics and hence in their imaging efficacy, which is not yet fully established.

The scientific interest in the field of magnetic carriers has shifted from colloidal suspensions of coated ferromagnetic NPs, forming aggregates sized between 7 and 200 nm, to multicomponent nanocapsules produced by self-assembly of molecular components in which magnetic and/or metal NPs constitute key components [60, 190, 191]. General aspects such as particle size, morphology, composition, chemical structure and processing methodology will determine the capsule mechanical properties and, finally, the performance [192, 193]. New interactions are expected to appear within

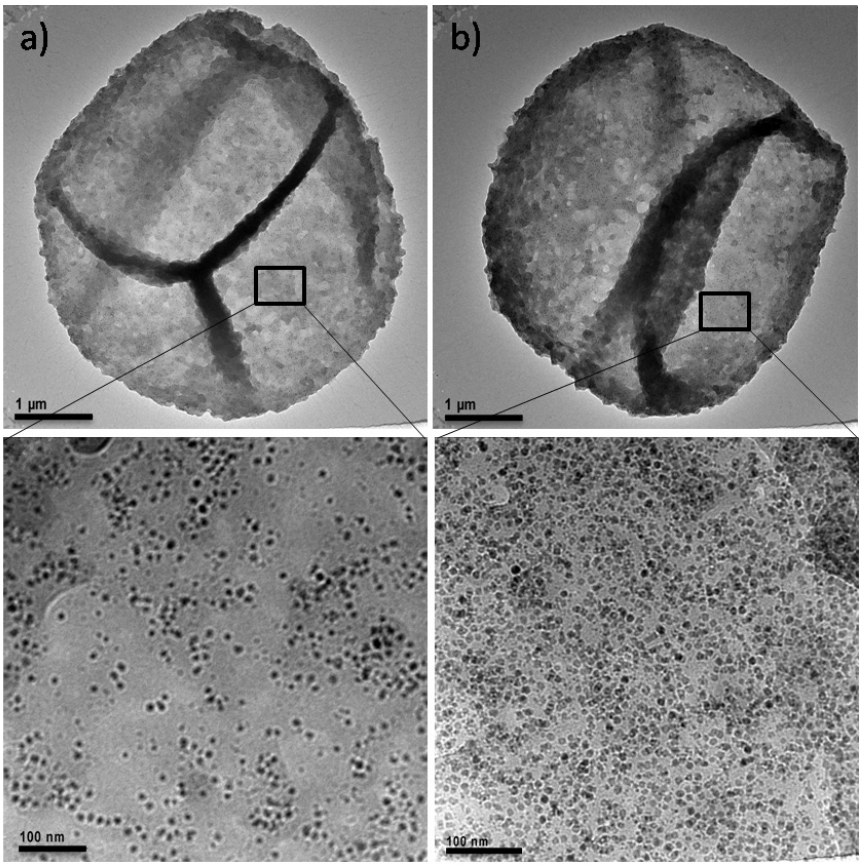

Figure 12. TEM images of iron oxide NPs encapsulated into the walls of polyelectrolyte capsules. (a) Capsules with a low concentration of γ-Fe_2O_3. (b) Capsules with a high concentration of γ-Fe_2O_3 NPs. The upper row shows low-magnification images of an individual capsule. The lower row shows high-resolution images zoomed into the capsule wall showing the distribution of the γ-Fe_2O_3 particles in the capsule wall. The scale bars in the upper and lower row correspond to 1 μm and 100 nm, respectively. (Reproduced with permission from [58]. Copyright 2011 American Chemical Society.)

the different components inside these systems and with the surroundings.

Among the important parameters that influence the relaxivity, the distance between the magnetic particles and external water molecules plays a key role. For example, proton transverse relaxivity measured for LbL-encapsulated Au–Fe_2O_3 and Au–$CoFe_2O_4$ DNA template nanostructures decreased significantly when compared to relaxivity for bare nanostructures [194]. On the other hand, aggregation of magnetic NPs into micelles has been shown to enhance NMR relaxivity in spite of the fact that water accessibility is reduced due to the reduction in specific surface area [195, 196]. Recently, MRI results of FePt NPs encapsulated into the walls of polyelectrolyte multilayer capsules have shown that the relaxivity increases as the FePt concentration increases [57] whereas the contrary occurs for γ-Fe_2O_3; the relaxivity decreases as the NPs concentration increases [58].

The magnetic and relaxivity responses of iron oxide NPs incorporated into the walls of polyelectrolyte multilayer capsules (see figure 12) has been investigated by Abbasi *et al* [58]. This configuration differs from that of particles embedded into a volume which are virtually equivalent with respect to their interaction with water protons. Therefore, these different configurations offer a unique opportunity for understanding the relationship between water accessibility and intrinsic relaxivity of the entrapped particles, which depend finally on their magnetic properties.

By considering the ensemble of NPs as interacting macrospins, Abbasi *et al* [58] performed the calculation of the average dipolar field. The authors found that the absolute value of the dipolar field averaged over the overall space was smaller for the capsule than for the uniformly distributed ensemble, leading to a smaller r_2 value for the former. Ensembles of free NPs have low packing densities and are in the regime of individual energy barriers; therefore, the T_B decreases as a function of packing fraction. On the other hand, NPs on capsules have locally large packing densities and their behaviour belongs to the regime of collective energy barriers. Consequently, the T_B increases with concentration. The latter is also true for aggregated arrays of NPs such as those present in commercial samples, where the packing density is high; however, in these cases, the T_B as well as the r_2 values increase with concentration, as observed in figure 13. Aggregation affects the spatially inhomogeneous particle distribution, leading to collective magnetization.

From these results it is clear that the geometrical layout of magnetic NPs also plays a role as important as the magnetic, structural or colloidal properties of the particles (magnetic saturation, anisotropy, homogeneous size and aggregate size). For low NP concentrations, relaxivity values are comparable

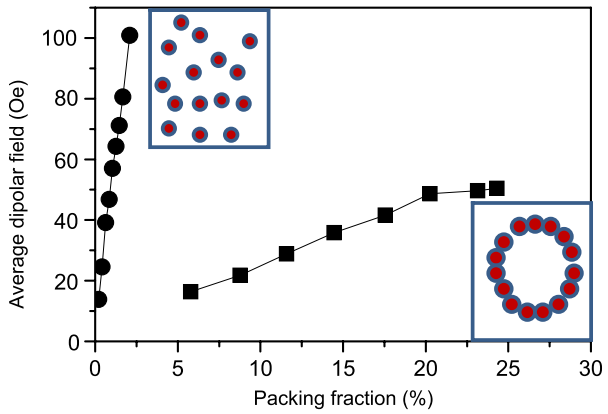

Figure 13. Average absolute value of the dipolar field in modelled systems as a function of the packing fraction. (● free NPs and ■ NPs in capsules). (Reproduced with permission from [58]. Copyright 2011 American Chemical Society.)

for both free and encapsulated NPs. However, for high NP concentrations, the NP arrangement on the capsule wall leads to a minimization of the dipolar energy, favouring a magnetization distribution parallel to the surface. This fact, together with lower water accessibility due to the increase in the distance between magnetic capsules at the same Fe concentration, results in lower relaxivity values (see table 1 in [58]).

The design of complex materials that serve simultaneously as diagnostic and therapeutic agents requires the optimization of each component. Thus, for example, capsules for drug delivery would be better if they contain large quantities of magnetic NPs to produce an efficient local heating under an AMF [12]. However, in the light of these results, NMR imaging contrast produced by this system would be diminished if the particles were encapsulated at high packing density in the capsule wall. NPs with larger magnetic anisotropy could enhance the image contrast.

5. Conclusions

For systems close to ferromagnetic instability, such as Pd and Pt, the size reduction is enough to produce an increase in $N(\varepsilon_F)$ due to the surface atom contributions. However, for materials that have diamagnetic behaviour in bulk, such as metallic Au or semiconductor ZnO, ferromagnetic-like behaviour at RT can be induced if the size is reduced to the nanoscale and the NPs are coated by organic surfactants.

The nature of the interactions between the surface atoms and the organic surfactant is also relevant for the onset of ferromagnetic-like behaviour. For instance, thiol bonded covalently to Au NPs induces permanent magnetic moments associated with the spin of the extra d charge localized near the Au–S bonds. The strong spin–orbit coupling of Au, associated with a high local anisotropy, may freeze the magnetic moments along the local easy axis and give rise to the appearance of permanent magnetism at the NP scale.

Similar behaviour has been observed in thiol or amine coated ZnO NPs with a magnetic moment per surface atom of 2×10^{-3} μ_B and 0.5×10^{-3} μ_B, respectively. A correlation in the evolution of the electronic structure, which is modified by the capping molecule, with the magnetic response of the sample is observed in ZnO NPs. Those NPs showing the highest XANES absorption (thiol) also exhibit the highest magnetic moment. From this study two conclusions can be derived: (a) a magnetic moment is induced in ZnO independently of the presence of ferromagnetic impurities and (b) this component comes from the modification of the electronic structure induced by the capping molecules.

It can be concluded that the anomalous magnetism observed in NPs which are far from ferromagnetic instability has its source at the NP surface and its contribution decreases as the size of the NP increase. Its strength can be modified by tuning the interactions of the surface atoms and the coating molecules. Although the intrinsic origin is not well understood, the use of selective techniques, such as Mossbauer and XMCD, has neatly indicated that the magnetism is intrinsic to the NP atoms.

The coating of ferromagnetic NPs such as FePt and Fe_3O_4 by inorganic shell-like Au or SiO_2 can enhance the physical and chemical properties of the core, making these nanostructures useful in applications otherwise inaccessible to their single-component counterpart. For instance, coating FePt by an Au shell improves the biological applications, whereas a SiO_2 shell additionally offers a platform to obtain thermal stabilized FePt NPs in the hard magnetic phase. Silica coatings of iron oxides can improve water stability since the silica surface provides additional steric repulsion. By coating magnetic NPs with silica, the biocompatibility can be improved and cellular damage can be induced in incubated HeLa cells by applying an AMF. However, the interaction at the core–shell interface plays a relevant role in the modification of the magnetic properties. The organic coatings of magnetic NPS can in addition improve the colloidal properties and sample biocompatibility; however, they could bear on the heating efficiency, since magnetic properties can be altered by the formation of the chemical bonds at the NP surface or the formation of different aggregates. The Brownian relaxation time and, consequently, the heating efficiency are affected also by the organic coating due to the increase of the hydrodynamic particle size.

On the other hand, the average dipolar field produced by ferromagnetic NPs encapsulated into the walls of polyelectrolyte multilayer capsules of microsize depends not only on the magnetic, structural or colloidal properties of the particles (magnetic saturation, anisotropy, homogeneous size and aggregate size) but also on the geometrical layout of the magnetic NPs.

In summary, it has been well established that selective coating of NPs provides an excellent way of controlling their magnetic properties and tailoring their characteristics for applications.

Acknowledgments

This work was supported by grants from the Spanish Ministry of Science and Innovation (MAT2009-14741-C02-00, CSD2007-00010) and the Madrid regional government CM (S009/MAT-1726).

References

[1] Sun S H, Murray C B, Weller D, Folks L and Moser A 2000 *Science* **287** 1989
[2] Bonder M J, Huang Y and Hadjipanayis G C 2005 Magnetic nanoparticles *Advanced Magnetic Nanostructures* ed D S A R Skomski (Berlin: Springer) p 183
[3] Terris B D and Thomson T 2005 *J. Phys. D: Appl. Phys.* **38** R199
[4] Hadjipanayis C G, Bonder M J, Balakrishanan S, Wang X, Mao H and Hadjipanayis G C 2008 *Small* **4** 1925
[5] Jin Y, Jia C, Huang S-W, O'Donnell M and Gao X 2010 *Nature Commun.* **1** 41
[6] John R, Rezaeipoor R, Adie S G, Chaney E J, Oldenburg A L, Marjanovic M, Haldar J P, Sutton B P and Boppart S A 2010 *Proc. Natl Acad. Sci. USA* **107** 8085
[7] Tsang S C, Caps V, Paraskevas I, Chadwick D and Thompsett D 2004 *Angew. Chem. Int. Edn* **43** 5645
[8] Lu A H, Schmidt W, Matoussevitch N, Bonnemann H, Spliethoff B, Tesche B, Bill E, Kiefer W and Schuth F 2004 *Angew. Chem. Int. Edn* **43** 4303
[9] Beveridge J S, Stephens J R and Williams M E 2011 *Analyst* **136** 2564
[10] Daniel M C and Astruc D 2004 *Chem. Rev.* **104** 293
[11] Roca A G, Costo R, Rebolledo A F, Veintemillas-Verdaguer S, Tartaj P, Gonzalez-Carreno T, Morales M P and Serna C J 2009 *J. Phys. D: Appl. Phys.* **42** 224002
[12] Pankhurst Q A, Thanh N K T, Jones S K and Dobson J 2009 *J. Phys. D: Appl. Phys.* **42** 224001
[13] Ortega D and Pankhurst Q A 2013 Magnetic hyperthermia *Nanostructures Through Chemistry* (*Nanoscience* vol 1) (Cambridge: The Royal Society of Chemistry) p 60
[14] Batlle X and Labarta A 2002 *J. Phys. D: Appl. Phys.* **35** R15
[15] Lu A H, Salabas E L and Schuth F 2007 *Angew. Chem. Int. Edn* **46** 1222
[16] Alivisatos A P 1996 *Science* **271** 933
[17] Yacaman M J, Marin M and Ascencio J A 2001 *J. Mol. Catal.* A **173** 13
[18] Billas I M L, Chatelain A and Deheer W A 1994 *Science* **265** 1682
[19] Pfandzelter R, Steierl G and Rau C 1995 *Phys. Rev. Lett.* **74** 3467
[20] Blugel S 1995 *Phys. Rev.* B **51** 2025
[21] Takano N, Kai T, Shiiki K and Terasaki F 1996 *Solid State Commun.* **97** 153
[22] Chen H, Brener N E and Callaway J 1989 *Phys. Rev.* B **40** 1443
[23] Alexandre S S, Anglada E, Soler J M and Yndurain F 2006 *Phys. Rev.* B **74** 054405
[24] Alexandre S S, Mattesini M, Soler J M and Yndurain F 2006 *Phys. Rev. Lett.* **96** 079701
[25] Rayl M, Wojtowic P J, Abrahams M S, Harvey R L and Buiocchi C J 1971 *Phys. Lett.* A **A 36** 477
[26] Del Bianco L, Hernando A, Bonetti E and Navarro E 1997 *Phys. Rev.* B **56** 8894
[27] Herr U, Jing J, Birringer R, Gonser U and Gleiter H 1987 *Appl. Phys. Lett.* **50** 472
[28] Cox A J, Louderback J G and Bloomfield L A 1993 *Phys. Rev. Lett.* **71** 923
[29] Garcia M A, Ruiz-Gonzalez M L, de la Fuente G F, Crespo P, Gonzalez J M, Llopis J, Gonzalez-Calbet J M, Vallet-Regi M and Hernando A 2007 *Chem. Mater.* **19** 889
[30] Sampedro B, Crespo P, Hernando A, Litran R, Lopez J C S, Cartes C L, Fernandez A, Ramirez J, Calbet J G and Vallet M 2003 *Phys. Rev. Lett.* **91** 237203
[31] Vager Z, Carmeli I, Leitus G, Reich S and Naaman R 2004 *J. Phys. Chem. Solids* **65** 713
[32] Garcia M A *et al* 2007 *Nano Lett.* **7** 1489
[33] Litran R, Sampedro B, Rojas T C, Multigner M, Sanchez-Lopez J C, Crespo P, Lopez-Cartes C, Garcia M A, Hernando A and Fernandez A 2006 *Phys. Rev.* B **73** 054404
[34] Crespo P, Litran R, Rojas T C, Multigner M, de la Fuente J M, Sanchez-Lopez J C, Garcia M A, Hernando A, Penades S and Fernandez A 2004 *Phys. Rev. Lett.* **93** 087204
[35] Guerrero E, Munoz-Marquez M A, Garcia M A, Crespo P, Fernandez-Pinel E, Hernando A and Fernandez A 2008 *Nanotechnology* **19** 17501
[36] Guerrero E, Rojas T C, Multigner M, Crespo P, Munoz-Marquez M A, Garcia M A, Hernando A and Fernandez A 2007 *Acta Mater.* **55** 1723
[37] Yamamoto Y, Miura T, Suzuki M, Kawamura N, Miyagawa H, Nakamura T, Kobayashi K, Teranishi T and Hori H 2004 *Phys. Rev. Lett.* **93** 116801
[38] Negishi Y, Tsunoyama H, Suzuki M, Kawamura N, Matsushita M M, Maruyama K, Sugawara T, Yokoyama T and Tsukuda T 2006 *J. Am. Chem. Soc.* **128** 12034
[39] Garitaonandia J S *et al* 2008 *Nano Lett.* **8** 661
[40] de la Venta J, Pinel E F, Crespo P, Garcia M A and Hernando A 2009 *Sci. Adv. Mater.* **1** 241
[41] Munoz-Marquez M A, Guerrero E, Fernandez A, Crespo P, Hernando A, Lucena R and Conesa J C 2010 *J. Nanopart. Res.* **12** 1307
[42] de la Presa P, Multigner M, de la Venta J, Garcia M A and Ruiz-Gonzalez M L 2006 *J. Appl. Phys.* **100** 123915
[43] Hori H, Yamamoto Y, Iwamoto T, Miura T, Teranishi T and Miyake M 2004 *Phys. Rev.* B **69** 174411
[44] Rueda T, de la Presa P and Hernando A 2007 *Solid State Commun.* **142** 676
[45] Hernando A, Crespo P and Garcia M A 2006 *Phys. Rev. Lett.* **96** 057206
[46] Hernando A, Crespo P, Garcia M A, Pinel E F, de la Venta J, Fernandez A and Penades S 2006 *Phys. Rev.* B **74** 052403
[47] Hernando A, Crespo P, Garcia M A, Coey M, Ayuela A and Echenique P M 2011 *Phys. Status Solidi* b **248** 2352
[48] Ayuela A, Crespo P, Garcia M A, Hernando A and Echenique P M 2012 *New J. Phys.* **14** 013064
[49] Hernando A and Garcia M A 2011 *J. Nanopart. Res.* **13** 5595
[50] de la Presa P, Multigner M, Morales M P, Rueda T, Fernandez-Pinel E and Hernando A 2007 *J. Magn. Magn. Mater.* **316** E753
[51] Yano K, Nandwana V, Chaubey G S, Poudyal N, Kang S, Arami H, Griffis J and Liu J P 2009 *J. Phys. Chem.* C **113** 13088
[52] Villanueva A, de la Presa P, Alonso J M, Rueda T, Martinez A, Crespo P, Morales M P, Gonzalez-Fernandez M A, Valdes J and Rivero G 2010 *J. Phys. Chem.* C **114** 1976
[53] Hartling T *et al* 2010 *Appl. Phys. Lett.* **96** 183111
[54] Figueroa S J A, Stewart S J, Rueda T, Hernando A and de la Presa P 2011 *J. Phys. Chem.* C **115** 5500
[55] Salado J, Insausti M, Lezama L, de Muro I G, Moros M, Pelaz B, Grazu V, de la Fuente J M and Rojo T 2012 *Nanotechnology* **23** 315102
[56] Hoskins C, Min Y, Gueorguieva M, McDougall C, Volovick A, Prentice P, Wang Z G, Melzer A, Cuschieri A and Wang L J 2012 *J. Nanobiotechnol.* **10** 27
[57] Morales M P *et al* 2009 *J. Mater. Chem.* **19** 6381
[58] Abbasi A Z *et al* 2011 *J. Phys. Chem.* C **115** 6257
[59] de la Presa P, Luengo Y, Multigner M, Costo R, Morales M P, Rivero G and Hernando A 2012 *J. Phys. Chem.* C **116** 25602–10
[60] de la Presa P, Rueda T, Morales M D, Chichon F J, Arranz R, Valpuesta J M and Hernando A 2009 *J. Phys. Chem.* B **113** 3051

[61] de la Presa P, Rueda T, Morales M P and Hernando A 2008 *IEEE Trans. Magn.* **44** 2816
[62] Shinohara T, Sato T and Taniyama T 2003 *Phys. Rev. Lett.* **91** 197201
[63] Gambardella P *et al* 2003 *Science* **300** 1130
[64] Jose-Yacaman M, Marin-Almazo M and Ascencio J A 2001 *J. Mol. Catal.* A **173** 61
[65] Cox A J, Louderback J G, Apsel S E and Bloomfield L A 1994 *Phys. Rev.* B **49** 12295
[66] Moruzzi V L and Marcus P M 1989 *Phys. Rev.* B **39** 471
[67] Sakamoto Y, Oba Y, Maki H, Suda M, Einaga Y, Sato T, Mizumaki M, Kawamura N and Suzuki M 2011 *Phys. Rev.* B **83** 104420
[68] Zhang H T, Ding J and Chow G M 2008 *Langmuir* **24** 375
[69] Coronado E, Ribera A, Garcia-Martinez J, Linares N and Liz-Marzan L M 2008 *J. Mater. Chem.* **18** 5682
[70] Sharma S, Kim B and Lee D 2012 *Langmuir* **28** 15958
[71] Kulriya P K, Mehta B R, Agarwal D C, Kumar P, Shivaprasad S M, Pivin J C and Avasthi D K 2012 *J. Appl. Phys.* **112** 014318
[72] Taniyama T, Ohta E and Sato T 1997 *Europhys. Lett.* **38** 195
[73] Hori H, Teranishi T, Nakae Y, Seino Y, Miyake M and Yamada S 1999 *Phys. Lett.* A **263** 406
[74] Reetz M T and Maase M 1999 *Adv. Mater.* **11** 773
[75] Guerrero E, Munoz-Marquez M A, Fernandez-Pinel E, Crespo P, Hernando A and Fernandez A 2008 *J. Nanopart. Res.* **10** 179
[76] Suber L, Fiorani D, Scavia G, Imperatori P and Plunkett W R 2007 *Chem. Mater.* **19** 1509
[77] Dutta P, Pal S, Seehra M S, Anand M and Roberts C B 2007 *Appl. Phys. Lett.* **90** 213102
[78] Brust M, Walker M, Bethell D, Schiffrin D J and Whyman R 1994 *J. Chem. Soc. Chem. Commun.* 801
[79] Teranishi T, Kiyokawa I and Miyake M 1998 *Adv. Mater.* **10** 596
[80] Leff D V, Brandt L and Heath J R 1996 *Langmuir* **12** 4723
[81] Papaconstantopoulous D A 1986 *Handbook of Band Structure of Elemental Solids* (New York: Plenum)
[82] Vogt E 1969 *Magnetism and Metallurgy* (New York: Academic)
[83] Zhang P, Kim P S and Sham T K 2003 *Appl. Phys. Lett.* **82** 1470
[84] Zhang P and Sham T K 2002 *Appl. Phys. Lett.* **81** 736
[85] Zhang P and Sham T K 2003 *Phys. Rev. Lett.* **90** 245502
[86] Skomski R and Coey J M D 1999 *Permanent Magnetism* (Bristol: Institute of Physics) chapter 3
[87] Hovel H, Fritz S, Hilger A, Kreibig U and Vollmer M 1993 *Phys. Rev.* B **48** 18178
[88] Kreibig U and Völlmer M 1995 *Optical Properties of Metal Clusters* (Berlin: Springer)
[89] Garcia M A, de la Venta J, Crespo P, Llopis J, Penades S, Fernandez A and Hernando A 2005 *Phys. Rev.* B **72** 241403
[90] Templeton A C, Chen S W, Gross S M and Murray R W 1999 *Langmuir* **15** 66
[91] Bain C D, Troughton E B, Tao Y T, Evall J, Whitesides G M and Nuzzo R G 1989 *J. Am. Chem. Soc.* **111** 321
[92] de la Fuente J M, Alcantara D, Eaton P, Crespo P, Rojas T C, Fernandez A, Hernando A and Penades S 2006 *J. Phys. Chem.* B **110** 13021
[93] Crespo P, Garcia M A, Pinel E F, Multigner M, Alcantara D, de la Fuente J M, Penades S and Hernando A 2006 *Phys. Rev. Lett.* **97** 177203
[94] de la Venta J *et al* 2009 *J. Nanosci. Nanotechnol.* **9** 6434
[95] Guerrero E, Munoz-Marquez M A, Fernandez A, Crespo P, Hernando A, Lucena R and Conesa J C 2010 *J. Appl. Phys.* **107** 064303
[96] Weare W W, Reed S M, Warner M G and Hutchison J E 2000 *J. Am. Chem. Soc.* **122** 12890
[97] Bartlett P A, Bauer B and Singer S J 1978 *J. Am. Chem. Soc.* **100** 5085
[98] Iwasa T and Nobusada K 2007 *Chem. Phys. Lett.* **441** 268
[99] Lopez-Acevedo O, Tsunoyama H, Tsukuda T, Hakkinen H and Aikens C M 2010 *J. Am. Chem. Soc.* **132** 8210
[100] Jadzinsky P D, Calero G, Ackerson C J, Bushnell D A and Kornberg R D 2007 *Science* **318** 430
[101] Heaven M W, Dass A, White P S, Holt K M and Murray R W 2008 *J. Am. Chem. Soc.* **130** 3754
[102] Alonso J A 2000 *Chem. Rev.* **100** 637
[103] Yourdshahyan Y and Rappe A M 2002 *J. Chem. Phys.* **117** 825
[104] Gonzalez C, Simon-Manso Y, Marquez M and Mujica V 2006 *J. Phys. Chem.* B **110** 687
[105] Luo W, Pennycook S J and Pantelides S T 2007 *Nano Lett.* **7** 3134
[106] Michael F, Gonzalez C, Mujica V, Marquez M and Ratner M A 2007 *Phys. Rev.* B **76** 224409
[107] Puerta L, Franco H J, Murgich J, Gonzalez C, Simon-Manso Y and Mujica V 2008 *J. Phys. Chem.* A **112** 9771
[108] Vager Z and Naaman R 2004 *Phys. Rev. Lett.* **92** 087205
[109] Carmeli I, Leitus G, Naaman R, Reich S and Vager Z 2003 *J. Chem. Phys.* **118** 10372
[110] Reich S, Leitus G and Feldman Y 2006 *Appl. Phys. Lett.* **88** 222502
[111] Hernando A and Garcia M A 2006 *Phys. Rev. Lett.* **96** 029703
[112] Garcia M A, Pinel E F, de la Venta J, Quesada A, Bouzas V, Fernandez J F, Romero J J, Martin-Gonzalez M S and Costa-Kramer J L 2009 *J. Appl. Phys.* **105** 013925
[113] Quesada A, Garcia M A, de la Venta J, Pinel E F, Merino J M and Hernando A 2007 *Eur. Phys. J.* B **59** 457
[114] Coey J M D and Chambers S A 2008 *MRS Bull.* **33** 1053
[115] Sharma P, Gupta A, Rao K V, Owens F J, Sharma R, Ahuja R, Guillen J M O, Johansson B and Gehring G A 2003 *Nature Mater.* **2** 673
[116] Pearton S J, Norton D P, Ip K, Heo Y W and Steiner T 2005 *Prog. Mater. Sci.* **50** 293
[117] Lee H J, Jeong S Y, Cho C R and Park C H 2002 *Appl. Phys. Lett.* **81** 4020
[118] Fukumura T, Jin Z W, Kawasaki M, Shono T, Hasegawa T, Koshihara S and Koinuma H 2001 *Appl. Phys. Lett.* **78** 958
[119] Ohno H 1998 *Science* **281** 951
[120] Dietl T, Ohno H, Matsukura F, Cibert J and Ferrand D 2000 *Science* **287** 1019
[121] Garcia M A *et al* 2005 *Phys. Rev. Lett.* **94** 217206
[122] Venkatesan M, Fitzgerald C B, Lunney J G and Coey J M D 2004 *Phys. Rev. Lett.* **93** 177206
[123] Van de Walle C G and Neugebauer J 2003 *Nature* **423** 626
[124] Lawes G, Risbud A S, Ramirez A P and Seshadri R 2005 *Phys. Rev.* B **71** 045201
[125] Kulkarni S K 2004 *Encyclopedia of Nanoscience and Nanotechnology* vol 2 (Valencia: American Scientific) p 537
[126] Sundaresan A, Bhargavi R, Rangarajan N, Siddesh U and Rao C N R 2006 *Phys. Rev.* B **74** 161306
[127] Kittilstved K R, Norberg N S and Gamelin D R 2005 *Phys. Rev. Lett.* **94** 147209
[128] Singh S B, Limaye M V, Date S K and Kulkarni S K 2008 *Chem. Phys. Lett.* **464** 208
[129] 2007 Research highlights *Nature Mater.* **6** 470
[130] Chaboy J *et al* 2010 *Phys. Rev.* B **82** 064411
[131] Guglieri C and Chaboy J 2010 *J. Phys. Chem.* C **114** 19629
[132] Forker M, de la Presa P, Hoffbauer W, Schlabach S, Bruns M and Szabo D V 2008 *Phys. Rev.* B **77** 054108
[133] Taylor M A, Alonso R E, Errico L A, Lopez-Garcia A, de la Presa P, Svane A and Christensen N E 2010 *Phys. Rev.* B **82** 165203

[134] Taylor M A, Alonso R E, Errico L A, Lopez-Garcia A, de la Presa P, Svane A and Christensen N E 2012 *Phys. Rev.* B **85** 155202
[135] Sundaresan A and Rao C N R 2009 *Nano Today* **4** 96
[136] Osorio-Guillen J, Lany S, Barabash S V and Zunger A 2006 *Phys. Rev. Lett.* **96** 107203
[137] Yoon S D, Chen Y, Yang A, Goodrich T L, Zuo X, Arena D A, Ziemer K, Vittoria C and Harris V G 2006 *J. Phys.: Condens. Matter* **18** L355
[138] Rumaiz A K, Ali B, Ceylan A, Boggs M, Beebe T and Shah S I 2007 *Solid State Commun.* **144** 334
[139] Zhao Q, Wu P, Li B L, Lu Z M and Jiang E Y 2008 *J. Appl. Phys.* **104** 073911
[140] Coey J M D, Stamenov P, Gunning R D, Venkatesan M and Paul K 2010 *New J. Phys.* **12** 053025
[141] Coey J M D, Venkatesan M and Fitzgerald C B 2005 *Nature Mater.* **4** 173
[142] Sanchez N, Gallego S and Munoz M C 2008 *Phys. Rev. Lett.* **101** 067206
[143] Hernando A *et al* 2011 *J. Phys.: Conf. Ser.* **292** 012005
[144] Tempere J, Silvera I F and Devreese J T 2002 *Phys. Rev.* B **65** 195418
[145] Kumar C S S R and Mohammad F 2010 *J. Phys. Chem. Lett.* **1** 3141
[146] Pazos-Perez N, Rodriguez-Gonzalez B, Hilgendorff M, Giersig M and Liz-Marzan L M 2010 *J. Mater. Chem.* **20** 61
[147] Seemann K M *et al* 2013 *Nanoscale* **5** 2511
[148] Ho D, Sun X L and Sun S H 2011 *Acc. Chem. Res.* **44** 875
[149] de la Presa P, Rueda T, Hernando A, Ramallo-Lopez J M, Giovanetti L J and Requejo F G 2008 *J. Appl. Phys.* **103** 103909
[150] Delalande M, Marcoux P R, Reiss P and Samson Y 2007 *J. Mater. Chem.* **17** 1579
[151] Wu J J, Hou Y L and Gao S 2011 *Nano Res.* **4** 836
[152] Stoner E C and Wohlfarth E P 1991 *IEEE Trans. Magn.* **27** 3475
[153] Verges M A, Costo R, Roca A G, Marco J F, Goya G F, Serna C J and Morales M P 2008 *J. Phys. D: Appl. Phys.* **41** 134003
[154] Goya G F, Berquo T S, Fonseca F C and Morales M P 2003 *J. Appl. Phys.* **94** 3520
[155] Wang L Y, Luo J, Fan Q, Suzuki M, Suzuki I S, Engelhard M H, Lin Y H, Kim N, Wang J Q and Zhong C J 2005 *J. Phys. Chem.* B **109** 21593
[156] Mohammad F, Balaji G, Weber A, Uppu R M and Kumar C 2010 *J. Phys. Chem.* C **114** 19194
[157] Banerjee S, Raja S O, Sardar M, Gayathri N, Ghosh B and Dasgupta A 2011 *J. Appl. Phys.* **109** 123902
[158] Robinson I, Tung L D, Maenosono S, Walti C and Thanh N T K 2010 *Nanoscale* **2** 2624
[159] Pal S, Morales M, Mukherjee P and Srikanth H 2009 *Synthesis and Magnetic Properties of Gold Coated Iron Oxide Nanoparticles* (New York: AIP) p 07B504
[160] Iglesias-Silva E, Vilas-Vilela J L, López-Quintela M A, Rivas J, Rodríguez M and León L M 2010 *J. Non-Cryst. Solids* **356** 1233
[161] Wang X, Wang L, Lim I I S, Bao K, Mott D, Park H-Y, Luo J, Hao S and Zhong C-J 2009 *J. Nanosci. Nanotechnol.* **9** 3005
[162] Chen S, Wang L J, Duce S L, Brown S, Lee S, Melzer A, Cuschieri S A and Andre P 2010 *J. Am. Chem. Soc.* **132** 15022
[163] Hyun C, Dee D C, Korgel B A and de Lozane A 2007 *Nanotechnology* **18** 055704
[164] Lee D C, Mikulec F V, Pelaez J M, Koo B and Korgel B A 2006 *J. Phys. Chem.* B **110** 11160
[165] Colak L and Hadjipanayis G C 2009 *IEEE Trans. Magn.* **45** 4081
[166] Aslam M, Fu L, Li S and Dravid V P 2005 *J. Colloid Interface Sci.* **290** 444
[167] Yamamoto S, Tamada Y, Ono T and Takano M 2012 *Chem. Lett.* **41** 1581
[168] Gonzalez-Fernandez M A, Torres T E, Andres-Verges M, Costo R, de la Presa P, Serna C J, Morales M R, Marquina C, Ibarra M R and Goya G F 2009 *J. Solid State Chem.* **182** 2779
[169] Vogt C, Toprak M, Muhammed M, Laurent S, Bridot J-L and Müller R 2010 *J. Nanopart. Res.* **12** 1137
[170] Kim D H, Thai Y T, Nikles D E and Brazel C S 2009 *IEEE Trans. Magn.* **45** 64
[171] Kaman O *et al* 2009 *Nanotechnology* **20** 275610
[172] Epherre R, Duguet E, Mornet S, Pollert E, Louguet S, Lecommandoux S, Schatz C and Goglio G 2011 *J. Mater. Chem.* **21** 4393
[173] Atsarkin V A, Levkin L V, Posvyanskiy V S, Melnikov O V, Markelova M N, Gorbenko O Y and Kaul A R 2009 *Int. J. Hyperth.* **25** 240
[174] Natividad E, Castro M, Goglio G, Andreu I, Epherre R, Duguet E and Mediano A 2012 *Nanoscale* **4** 3954
[175] Asin L, Goya G F, Tres A and Ibarra M R 2013 *Cell Death Dis.* **4** e596
[176] Hergt R, Hiergeist R, Hilger I, Kaiser W A, Lapatnikov Y, Margel S and Richter U 2004 *J. Magn. Magn. Mater.* **270** 345
[177] Gupta A K and Gupta M 2005 *Biomaterials* **26** 3995
[178] Fortin J P, Wilhelm C, Servais J, Menager C, Bacri J C and Gazeau F 2007 *J. Am. Chem. Soc.* **129** 2628
[179] Laurent S, Dutz S, Häfeli U O and Mahmoudi M 2011 *Adv. Colloid Interface Sci.* **166** 8
[180] Asin L, Ibarra M R, Tres A and Goya G F 2012 *Pharm. Res.* **29** 1319
[181] Guardia P, Di Corato R, Lartigue L, Wilhelm C, Espinosa A, Garcia-Hernandez M, Gazeau F, Manna L and Pellegrino T 2012 *ACS Nano* **6** 3080
[182] Mehdaoui B, Meffre A, Carrey J, Lachaize S, Lacroix L M, Gougeon M, Chaudret B and Respaud M 2011 *Adv. Funct. Mater.* **21** 4573
[183] Gonzales-Weimuller M, Zeisberger M and Krishnan K M 2009 *J. Magn. Magn. Mater.* **321** 1947
[184] Levy M, Wilhelm C, Siaugue J M, Horner O, Bacri J C and Gazeau F 2008 *J. Phys.: Condens. Matter* **20** 204133
[185] Glockl G, Hergt R, Zeisberger M, Dutz S, Nagel S and Weitschies W 2006 *J. Phys.: Condens. Matter* **18** S2935
[186] Hergt R, Dutz S, Muller R and Zeisberger M 2006 *J. Phys.: Condens. Matter* **18** S2919
[187] Martinez-Boubeta C *et al* 2013 *Sci. Rep.* **3** 1652
[188] Costo R, Bello V, Robic C, Port M, Marco J F, Morales M P and Veintemillas-Verdaguer S 2012 *Langmuir* **28** 178
[189] Lacroix L M, Ho D and Sun S H 2010 *Curr. Top. Med. Chem.* **10** 1184
[190] Gorin D A, Portnov S A, Inozemtseva O A, Luklinska Z, Yashchenok A M, Pavlov A M, Skirtach A G, Mohwald H and Sukhorukov G B 2008 *Phys. Chem. Chem. Phys.* **10** 6899
[191] Salgueirino-Maceira V and Correa-Duarte M A 2007 *Adv. Mater.* **19** 4131
[192] Bedard M F, Munoz-Javier A, Mueller R, del Pino P, Fery A, Parak W J, Skirtach A G and Sukhorukov G B 2009 *Soft Matter* **5** 148
[193] Wang W, Pacheco V, Krause H-J, Zhang Y, Dong H, Hartmann R, Willbold D, Offenhäusser A and Gu Z 2012 *J. Phys. Chem.* C **116** 17880
[194] Jaganathan H, Gieseck R L and Ivanisevic A 2010 *J. Phys. Chem.* C **114** 22508
[195] Mulder W J M, Strijkers G J, van Tilborg G A F, Griffioen A W and Nicolay K 2006 *NMR Biomed.* **19** 142
[196] Seo S B, Yang J, Lee T I, Chung C H, Song Y J, Suh J S, Yoon H G, Huh Y M and Haam S 2008 *J. Colloid Interface Sci.* **319** 429